

**AFRL-ML-TY-TR-2002-4544**



## **Real-Time Fuel Vapor Detector**

**Greg Gillespie**

Dakota Technologies, Inc. (DTI)  
2201-A 12<sup>th</sup> St. N.  
Fargo, ND 58102

Approved for Public Release; Distribution Unlimited

**AIR FORCE RESEARCH LABORATORY  
MATERIALS & MANUFACTURING DIRECTORATE  
AIR EXPEDITIONARY FORCES TECHNOLOGIES DIVISION  
139 BARNES DRIVE, STE 2  
TYNDALL AFB FL 32403-5323**

**20020919 017**

## NOTICES

USING GOVERNMENT DRAWINGS, SPECIFICATIONS, OR OTHER DATA INCLUDED IN THIS DOCUMENT FOR ANY PURPOSE OTHER THAN GOVERNMENT PROCUREMENT DOES NOT IN ANY WAY OBLIGATE THE US GOVERNMENT. THE FACT THAT THE GOVERNMENT FORMULATED OR SUPPLIED THE DRAWINGS, SPECIFICATIONS, OR OTHER DATA DOES NOT LICENSE THE HOLDER OR ANY OTHER PERSON OR CORPORATION; OR CONVEY ANY RIGHTS OR PERMISSION TO MANUFACTURE, USE, OR SELL ANY PATENTED INVENTION THAT MAY RELATE TO THEM.

THIS REPORT IS RELEASABLE TO THE NATIONAL TECHNICAL INFORMATION SERVICE  
5285 PORT ROYAL RD.

SPRINGFIELD VA 22161

TELEPHONE 703 487 4650; 703 4874639 (TDD for the hearing-impaired)

E-MAIL [orders@ntis.fedworld.gov](mailto:orders@ntis.fedworld.gov)

WWW <http://www.ntis.gov/index.html>

AT NTIS, IT WILL BE AVAILABLE TO THE GENERAL PUBLIC, INCLUDING FOREIGN NATIONS.

THIS TECHNICAL REPORT HAS BEEN REVIEWED AND IS APPROVED FOR PUBLICATION.



DAVID M. KEMPISTY, Capt, USAF, BSC  
Program Manager

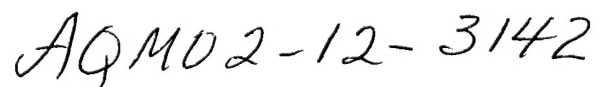


JEFFREY H. SANDERS  
Chief, Weapons Systems Logistics Branch



DONALD R. HUCKLE, JR., Colonel, USAF  
Chief, Air Expeditionary Forces Technologies Division

Do not return copies of this report unless contractual obligations or notice on a specific document requires its return.



# REPORT DOCUMENTATION PAGE

Form Approved  
OMB No. 0704-0188

Public reporting burden for this collection of information is estimated to average 1 hour per response, including the time for reviewing instructions, searching existing data sources, gathering and maintaining the data needed, and completing and reviewing the collection of information. Send comments regarding this burden estimate or any other aspect of this collection of information, including suggestions for reducing this burden, to Washington Headquarters Services, Directorate for Information Operations and Reports, 1215 Jefferson Davis Highway, Suite 1204, Arlington, VA 22202-4302, and to the Office of Management and Budget, Paperwork Reduction Project (0704-0188), Washington, DC 20503.

1. AGENCY USE ONLY (Leave blank)	2. REPORT DATE 1 July 2002	3. REPORT TYPE AND DATES COVERED Technical Report/ 990508-010531	
4. TITLE AND SUBTITLE Real-Time Fuel Vapor Detector		5. FUNDING NUMBERS Contract #: FO8637-99-C6005 JON: 300505D9 PE: SBIR PR: TA: WU:	
6. AUTHOR(S) Gillespie, Greg, PhD			
7. PERFORMING ORGANIZATION NAME(S) AND ADDRESS(ES) Dakota Technologies, Inc. (DTI) 2201-A 12 <sup>th</sup> St. N. Fargo, ND 58102		8. PERFORMING ORGANIZATION REPORT NUMBER	
9. SPONSORING/MONITORING AGENCY NAME(S) AND ADDRESS(ES) (Program Mgr Name & Ph #) AFRL/MLQL 139 Barnes Drive, Suite 2 Tyndall AFB, FL 3403-5323		10. SPONSORING/MONITORING AGENCY REPORT NUMBER AFRL-ML-TY-TR-2002-4544	
11. SUPPLEMENTARY NOTES Technical Monitor: Capt David M. Kempisty, AFRL/MLQL, 850-293-6126 Availability of this report is specified on the verso of front cover.			
12a. DISTRIBUTION/AVAILABILITY STATEMENT Distribution Unlimited.		12b. DISTRIBUTION CODE (Leave this block blank)	
13. ABSTRACT:  Report describes a resonance enhanced multiphoton ionization (REMPI) technique to measure vapor leakage from fuel tanks. The technique is a nonlinear optical process where two photons are simultaneously absorbed by an analyte resulting in the ejection of an electron to form a positively charged parent ion. Leak detector is comprised of three major components: a pulsed UV laser, an ionization cell, and electronics to convert the generated ion current to a measurable voltage.			
14. SUBJECT TERM REMPI, resonance enhanced multiphoton ionization, fuel vapor detector		15. NUMBER OF PAGES 46	
16. PRICE CODE			
17. SECURITY CLASSIFICATION OF REPORT UNCLASSIFIED	18. SECURITY CLASSIFICATION OF THIS PAGE UNCLASSIFIED	19. SECURITY CLASSIFICATION OF ABSTRACT UNCLASSIFIED	20. LIMITATION OF ABSTRACT SAR UL

## Table of Contents

Table of Contents .....	ii
List of Figures .....	iv
List of Tables.....	vi
Introduction .....	1
REMPI Technique.....	2
Description .....	2
Spectroscopic Data.....	2
System Development.....	6
Laser Options .....	6
Ionization Cell .....	6
Bias Studies .....	7
Electrode Length/Geometry Studies .....	8
Flow and Pressure Studies.....	10
Electronics Development .....	11
Calibration.....	12
Software and GPS .....	12
Laboratory Studies .....	13
Signal Dependence on Laser Energy .....	13
Fiber Optic Delivery of Laser Light.....	13
Semi-Permeable Membrane Studies .....	14
Sorbent Interface Studies .....	18
Dust Elimination .....	18
Responsivity of the Detector .....	19
Selectivity Towards Aromatic Hydrocarbons .....	23
Field Studies .....	26
Pipeline Leak Detection in Western North Dakota .....	26
Field Testing at Offutt Air Force Base.....	29
Field Testing near Lamesa Texas.....	30
Calibration Procedure.....	31
Soil Gas Analysis with Fuel Vapor Detector .....	31
Field Testing at Tinker Air Force Base .....	33

Calibration Procedure.....	33
Building 976.....	33
Building 230.....	36
Spin-Off Applications .....	41
Aromatic Specific Laser Ionization Detector.....	41
Chemical Warfare Agents .....	43
Oil and Gas Exploration.....	44
Fulfillment of Technical Objectives.....	44
Conclusions .....	45
References .....	46

## List of Figures

Figure 1. Absolute absorption spectra (A) and normalized absorption spectra (B) of benzene and toluene .....	3
Figure 2. Normalized laser absorbance spectra for benzene and toluene in the B-band region ....	4
Figure 3. REMPI spectrum of benzene vapor, expressed as total ion charge collected in Coulombs as a function of wavelength, acquired in 0.01 nm wavelength increments .....	5
Figure 4. REMPI spectrum of toluene vapor, expressed as total ion charge collected in Coulombs as a function of wavelength, acquired in 0.05 nm wavelength increments .....	5
Figure 5. Final version of REMPI cell. The inset shows an end-on view of the electrode geometry.....	7
Figure 6. Affect of varying bias voltage on observed REMPI waveform.....	8
Figure 7. Affect of electrode length and geometry on observed waveforms .....	9
Figure 8. Comparison of waveform maxima and waveform area (data based on Figure 7 waveforms).....	9
Figure 9. Pressure dependence of the REMPI cell .....	10
Figure 10. Flow rate dependence of the REMPI cell .....	11
Figure 11. Chromatographic elution of toluene comparing the integrator with the transimpedance amplifier .....	12
Figure 12. Quadratic dependence of signal on laser energy .....	13
Figure 13. Benzene REMPI signal, 667 ppb (fiber tip between electrodes) .....	14
Figure 14. REMPI response as toluene (2.6 ng) was eluted from the GC through the outer stainless steel tube with various airflow rates inside the membrane tube .....	15
Figure 15. Chromatogram peak areas (2.6 ng toluene injected on column) with varied flow rates inside the membrane tube.....	16
Figure 16. Incremental additions of toluene to water – sampling with silicone tube membrane (air flow = 25 mL/min).....	17
Figure 17. Calibration curve of toluene in water – sampling with silicone tube membrane.....	17
Figure 18. Toluene signals as a result of pre-concentration with a Tenax trap.....	18
Figure 19. Dust generator used to test different filtering systems.....	19
Figure 20. Response waveforms for 4.9 ppb toluene and background signal.....	20
Figure 21. Low concentration calibration curve for toluene .....	20
Figure 22. Higher concentration calibration curve for toluene .....	21
Figure 23. Chromatograms of toluene eluted from a GC column.....	21
Figure 24. Initial current integrator response for various toluene concentrations.....	22

Figure 25. Current integrator response with blank air and 1 ppm toluene standard gas The signal to noise ratio of 2300 for 1 ppm toluene implies a limit of detection of 1.3 ppb.....	22
Figure 26. Leak Detector and PID response to JP-4 injected on column.....	24
Figure 27. Leak Detector and PID response to JP-8 injected on column.....	24
Figure 28. Leak detector and PID response to gasoline (in hexanes) injected on column.....	25
Figure 29. Leak detector and PID response to a BTEX mixture in hexanes.....	26
Figure 30. Data collected at a leaking wet gas site .....	28
Figure 31. Data collected at a repaired crude oil leak site (north-south transects) .....	28
Figure 32. Different sampling strategies used at crude oil site .....	29
Figure 33. Leak detector and PID signals from the evaluation of an above-ground fuel pipeline with several joints and valves.....	30
Figure 34. Chemical structure of Trifluralin .....	33
Figure 35. Locations where fuel vapor detector measurements were taken in building 976.....	34
Figure 36. Fuel vapor detector logs in building 976 .....	35
Figure 37. Fuel vapor detector log in pneumdraulics room of building 230.....	37
Figure 38. Fuel vapor detector log in computer room/study lounge of building 230 .....	38
Figure 39. Fuel vapor detector log as E-3 is powered up. Also shown are logs as fuel vapor detector is moved around building 230.....	39
Figure 40. Fuel vapor detector log in building 230 after E-3 is powered down. ....	41
Figure 41. Sensitivity of ArSLID towards toluene .....	42
Figure 42. Selectivity advantage of ArSLID vs. PID for a mixture of aromatic and aliphatic hydrocarbons .....	43

## List of Tables

Table 1. Limits of detection for select BTEX and fuel components .....	23
Table 2. Summary of the results obtained by New Paradigm Explorations for benzene, toluene, ethylbenzene (e-benzene) and total xylenes in parts per billion (ppb). Sample location is in the left column and analyte is in top column.....	31
Table 3. Summary of analysis of samples (total aromatics in ppb toluene) collected near Lamesa Texas. The left column is sample location (Og = Ogallala) and the top row is sample type: bgs = below ground surface; 3" = 3" above ground; 2ft = 2 feet above ground; 8ft = 8 feet above ground; 8ftC = 8 feet above ground with carbon trap; 100ppb = 10:1 dilution of 1 ppmv toluene in air.....	32
Table 4. Summary of technical objectives and significance .....	45

## Introduction

Enormous quantities of bulk fuels (jet fuel, diesel, gasoline) are produced in refineries, transferred across the country through pipelines, stored and distributed from depots, and consumed by the military and commercial air carriers. Although not an immediate focus of this research program, gasoline consumption in personal vehicles and their supply from the ubiquitous corner gas station represents another huge, related industry. Because the Air Force probably handles more fuel than any single organization in the world, its personnel have major responsibility to:

- Ensure fuels pass quality standards
- Manage the logistics of storing and efficiently distributing the fuel
- Maintain fuel systems and tanks on aircraft
- Minimize fuel-related impacts on the environment
- Protect occupational safety of workers

Of course, eliminating any risk of fires or explosions is the pre-eminent consideration.

Methods that can measure low concentrations of fuel vapors more quickly and quantitatively than currently available instrumental approaches (e.g., gas chromatography, organic vapor analyzers, lower explosion limit monitors) are urgently needed. Each of the existing approaches is inadequate for one or more of the following reasons: low sensitivity, susceptibility to interferences, slow response, and complicated operational and/or maintenance requirements. By developing a user-friendly instrument that specifically responds to fuel hydrocarbons in the sub-ppmv range in less than one second, Dakota Technologies, Inc. (DTI) has overcome these limitations. As a consequence, the Air Force will be able to shift from a reactive mode (solving problems after they have become apparent) to a problem prevention mode.

The data presented in this report prove the potential of a pulsed laser photoionization detector that creates ions by the process known as resonance-enhanced multiphoton ionization (REMPI). For convenience we will refer to such instruments as Laser Ionization Detectors (LIDs), which can be contrasted with conventional photoionization detectors (PIDs) that use far-ultraviolet lamps to create the ions. With our collaborators at North Dakota State University (NDSU), DTI has researched REMPI methods for over 5 years and is strongly committed to being a leader in applying REMPI to "real-world" problems.

Of the baseline technologies for vapor sensing and analysis, LIDs most closely resemble organic vapor analyzers (OVAs), also known as organic vapor monitors (OVMs). An OVA is little more than a gas chromatography (GC) detector connected to a small pump. GC analysis involves sweeping the sample through the separation column with a carrier gas and detecting the compounds as they elute from the column at different and characteristic retention times. OVAs sacrifice the specificity of GC methods to gain very fast response, typically a few seconds. The beauty of our approach is that the laser provides the specificity without a column.

The advantages of the LID over an OVA-PID for purposes of fuel vapor detection include:

- Better sensitivity (by a projected factor of 5-10)
- Specific response to aromatic hydrocarbons (and therefore to fuels)
- Immunity to the humidity effects that strongly influence PID response
- Wider dynamic range

One can also contrast our approach with helium leak detectors or other tracer methods designed to probe for vapors outside a tank, pipeline, etc. The fact that the LID directly senses the actual fuel components, not added tracers, is greatly advantageous. Downtime during testing is avoided because the system remains in operation and the testing is carried out under actual operating conditions. Methods in which the test body must be emptied for testing or subjected to an overpressure suffer from changing conditions with possible varying leak properties.

## REMPI Technique

### Description

Multiphoton ionization is a nonlinear optical process where two photons are simultaneously absorbed by an analyte resulting in the ejection of an electron to form a positively charged parent ion. Since it requires the simultaneous absorption of two photons, the process is very unlikely to occur; however, the situation changes markedly if the energy of one of the photons corresponds to a resonant transition (absorption band) of the analyte. In this event, the process is known as resonance enhanced multiphoton ionization (REMPI). The enhancement in the efficiency is oftentimes several orders of magnitude higher for resonant versus nonresonant processes. Due to the dependence of the efficiency on the absorption spectra of the analytes, we performed an in-depth investigation of the spectroscopy of several aromatic compounds, benzene and toluene in particular.

### Spectroscopic Data

Initial investigations were the conventional absorption spectra of the analytes of interest. This experiment examined absorption near 266.8 nm (corresponding to the 4<sup>th</sup> harmonic of Nd:KGW) for a set of eight aromatic compounds including benzene, toluene, ethylbenzene, *o*-xylene, *m*-xylene, *p*-xylene, 1,2,4-trimethylbenzene, and 1,3,5-trimethylbenzene. This particular wavelength region is known for benzene as the B-band. Gas phase absorption spectra of these compounds between 266.4 and 267.2 nm were obtained with the Cary 500 spectrophotometer operated in independent mode to attain the narrowest bandwidth (0.01 nm) and minimal wavelength step size (0.005 nm) possible.

Figure 1 contains the spectra of benzene and toluene in this wavelength range, plotted both as absolute absorbance and as absorbance normalized to the respective maxima. Figure 1 highlights the extensive overlap of the spectra of benzene and toluene in this wavelength range. According to the data, both species absorb significantly upward from 266.6 nm to at least 267.2 nm. Spectra for the other compounds were essentially flat lines around 0.05 absorbance units indicating very broad absorbances in the region of interest. This strong resonances displayed by both benzene and toluene indicate that even in a complex mixture of alkylbenzenes it may be possible to discern the benzene and toluene concentrations.

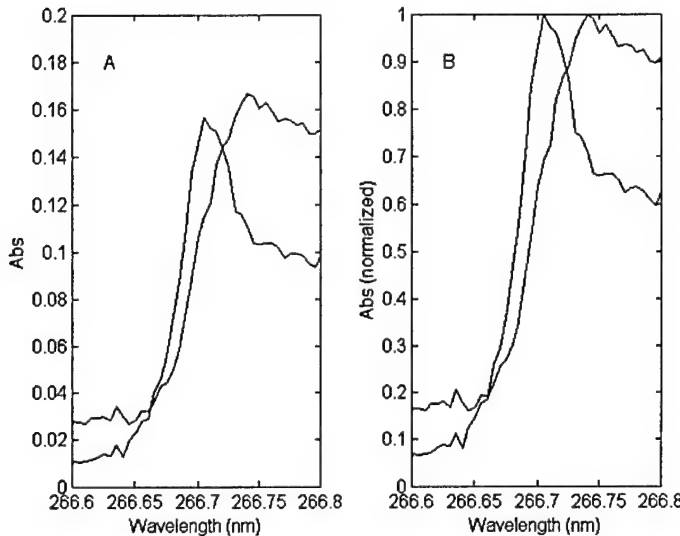


Figure 1. Absolute absorption spectra (A) and normalized absorption spectra (B) of benzene and toluene

To achieve higher resolution spectra we performed laser absorbance measurements of benzene and toluene. We used a tunable dye laser (the Northern Lights designed and built by DTI) which was pumped with the 3<sup>rd</sup> harmonic of Nd:YAG. Coumarin 500 was tuned from 500 to 540 nm. Frequency doubling provided light in the 250-270 nm wavelength range. Software to control the dye laser scanning and the absorbance data collection was written and has been extensively (and successfully) tested. Beam splitters and pyroelectric energy meters or photodiodes are placed before and after the gas cell to monitor the laser pulse energy with a digital storage oscilloscope. The spectra shown in Figure 2 give us the most accurate measurement of the wavelength difference between the benzene and toluene in the B-band region.

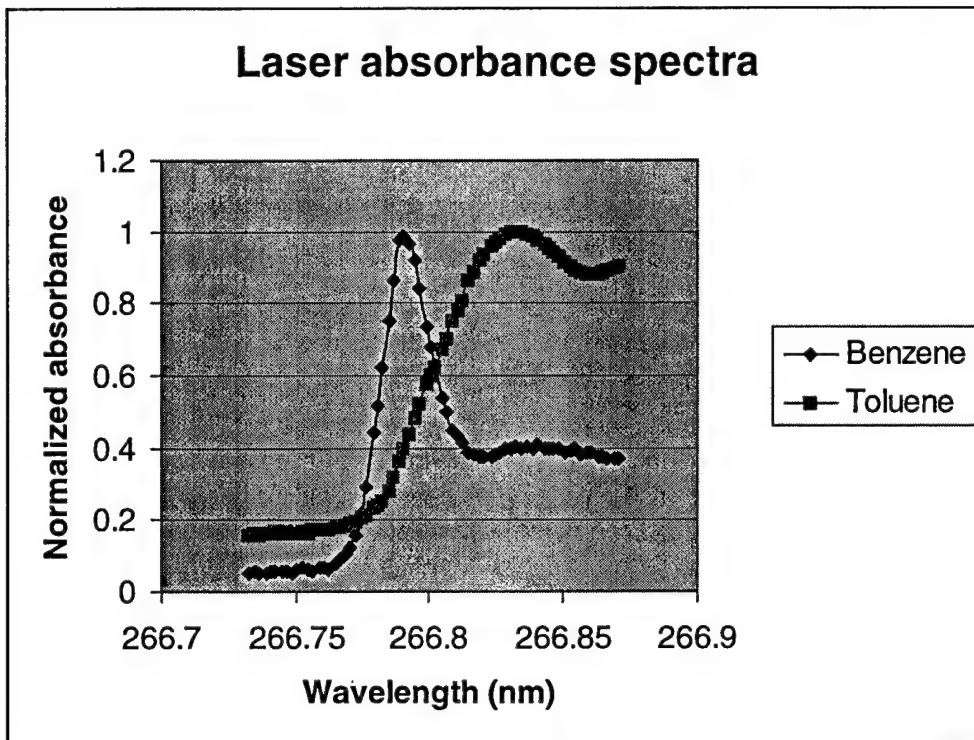


Figure 2. Normalized laser absorbance spectra for benzene and toluene in the B-band region

The final spectroscopic measurement was the REMPI signal as a function of wavelength. The frequency-tripled output of the Nd:YAG-pumped Ti:sapphire laser was used to perform REMPI of aromatic vapors within an ionization detector. The concentration of benzene in the detector was approximately 640 ppbV in room air (Figure 3). The toluene concentration was approximately 37 ppbV (Figure 4).

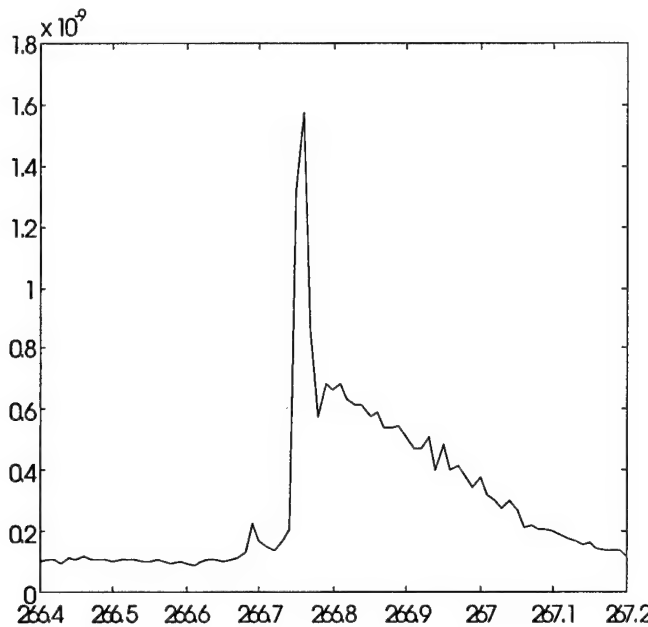


Figure 3. REMPI spectrum of benzene vapor, expressed as total ion charge collected in Coulombs as a function of wavelength, acquired in 0.01 nm wavelength increments

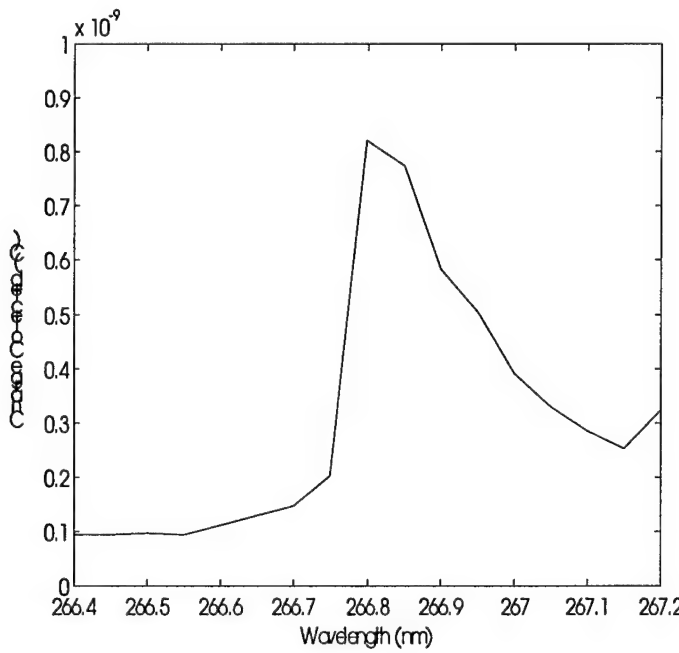


Figure 4. REMPI spectrum of toluene vapor, expressed as total ion charge collected in Coulombs as a function of wavelength, acquired in 0.05 nm wavelength increments

## System Development

Three major components comprise the leak detector: a pulsed ultraviolet laser, an ionization cell, and electronics to convert the generated ion current to a measurable voltage. Additional features of the system are a convenient means to calibrate the system to a toluene standard and a convenient user interface that includes a global positioning system.

### Laser Options

We had used the 4<sup>th</sup> harmonic (266 nm) of a Nd:YAG laser (Big Sky Ultra CFR) in Phase I research to demonstrate the feasibility of laser ionization to sensitively monitor fuel vapors in real-time.

In Phase II we proposed to investigate a number of laser options that would potentially offer a modest degree of tunability (a few nanometers) to allow differentiation between benzene, toluene, and other aromatic compounds measured. We ultimately chose Nd:KGW (neodymium doped into a potassium gadolinium tungstate crystal) as the preferred gain medium. The fundamental wavelength of Nd:KGW was measured to be 1067.156 nm which is converted to 266.789 nm by fourth harmonic generation. This wavelength coincides with strong absorbances of both toluene and benzene making it an excellent wavelength for REMPI.

Initially we contracted with Big Sky Laser Technology to substitute a Nd:KGW rod for a Nd:YAG rod in a customized Ultra CFR laser. This laser was flashlamp pumped and drew a considerable amount of power (several amps) that made it inconvenient for portable field use. We explored options for tuning the laser (including establishing a cooperative research and development agreement with the Navy SPAWAR) but ultimately determined that money would be better spent obtaining a laser with a lower power draw making it more convenient for field use.

We identified the DIVA laser by Thomson-CSF (now Thales) as a viable diode-pumped option that used a fraction of the power of the Ultra. Initially we used a Nd:YAG version of the laser to determine that it would be a viable substitute for the Ultra and ultimately had Thales incorporate a Nd:KGW rod *in lieu* of the Nd:YAG.

### Ionization Cell

There are many aspects of the ionization cell that were optimized en route to development of the final version shown in Figure 5. Elements that were optimized include the bias potential between the electrodes, electrode length and shape, and flow and pressure dependencies of the observed signal.

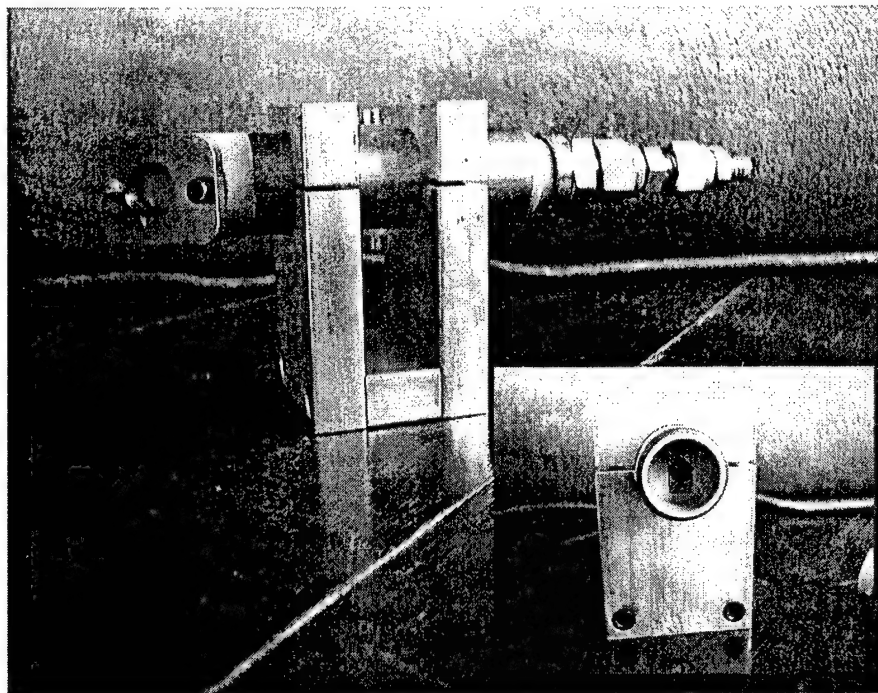


Figure 5. Final version of REMPI cell. The inset shows an end-on view of the electrode geometry.

### Bias Studies

In the REMPI cell there are two electrodes, one is held at ground (anode) while the other is at a negative potential (cathode). The potential difference between the electrodes is the bias voltage of the cell. Seven different bias voltages were applied to the cell (see Figure 6); combining high voltage batteries in series generated the voltages. As the bias voltage increased, the observed waveform (using a transimpedance amplifier) increased in amplitude and decreased in width. We chose to use a 300 V bias because it gave adequate signal strength and could be generated with a single commercially available battery.

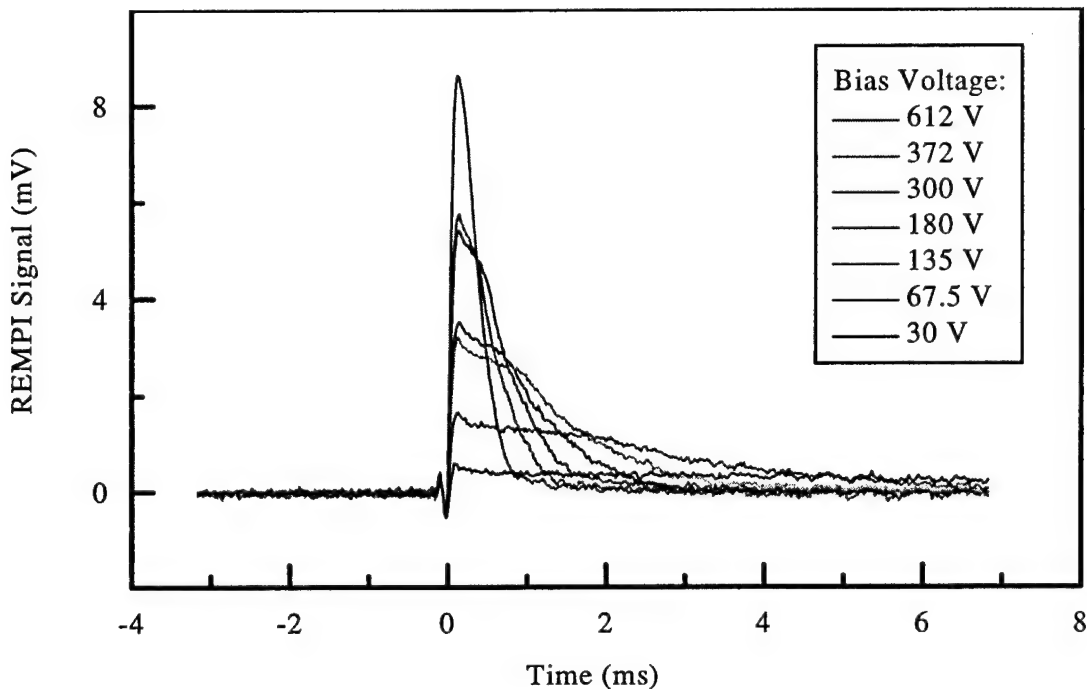


Figure 6. Affect of varying bias voltage on observed REMPI waveform

### Electrode Length/Geometry Studies

In designing the REMPI cell another parameter was the length and geometry of electrodes used. We hypothesized that longer electrodes would produce a larger signal since they increase the path-length where ionization occurs. This was born out by experiment (see Figure 7). Another factor is the geometry of the electrode. We wanted the cell to be capable of supporting a laminar flow of gas to facilitate more rapid response and minimize eddy-currents where analytes could be trapped. It was easiest to design the cell with a cylindrical bore that necessitated the use of curved electrodes. The curved electrodes produce a waveform that looks different from flat electrodes (see Figure 7), and gives a higher maximum value for its length (compared to flat electrodes), the waveform area falls right on line (see Figure 8).

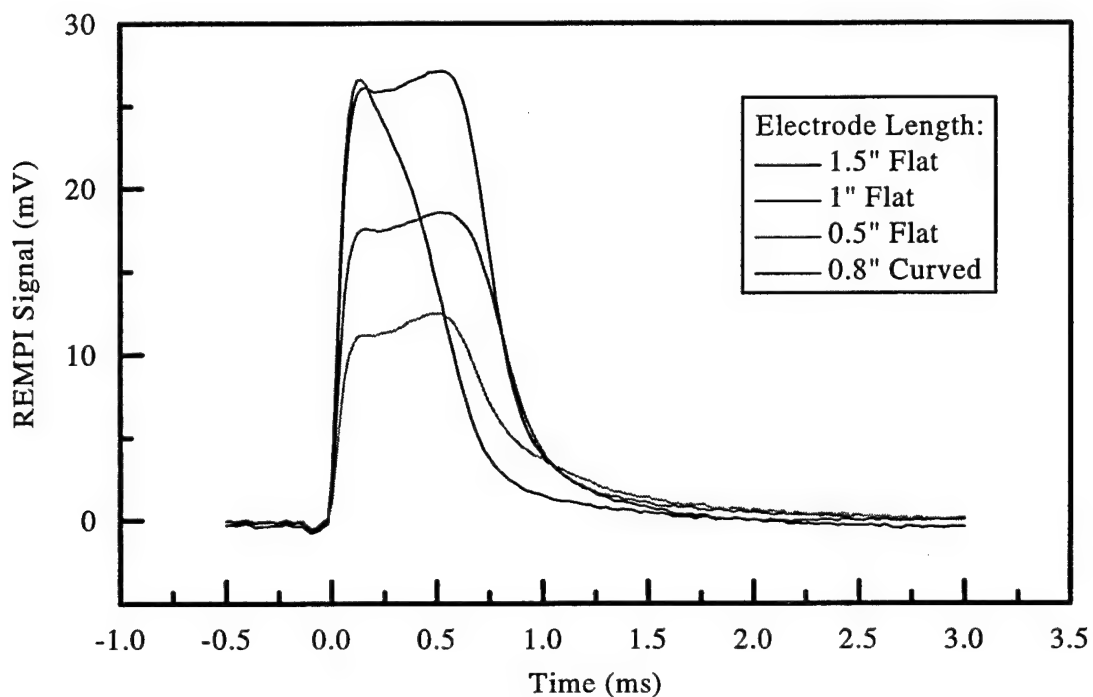


Figure 7. Affect of electrode length and geometry on observed waveforms

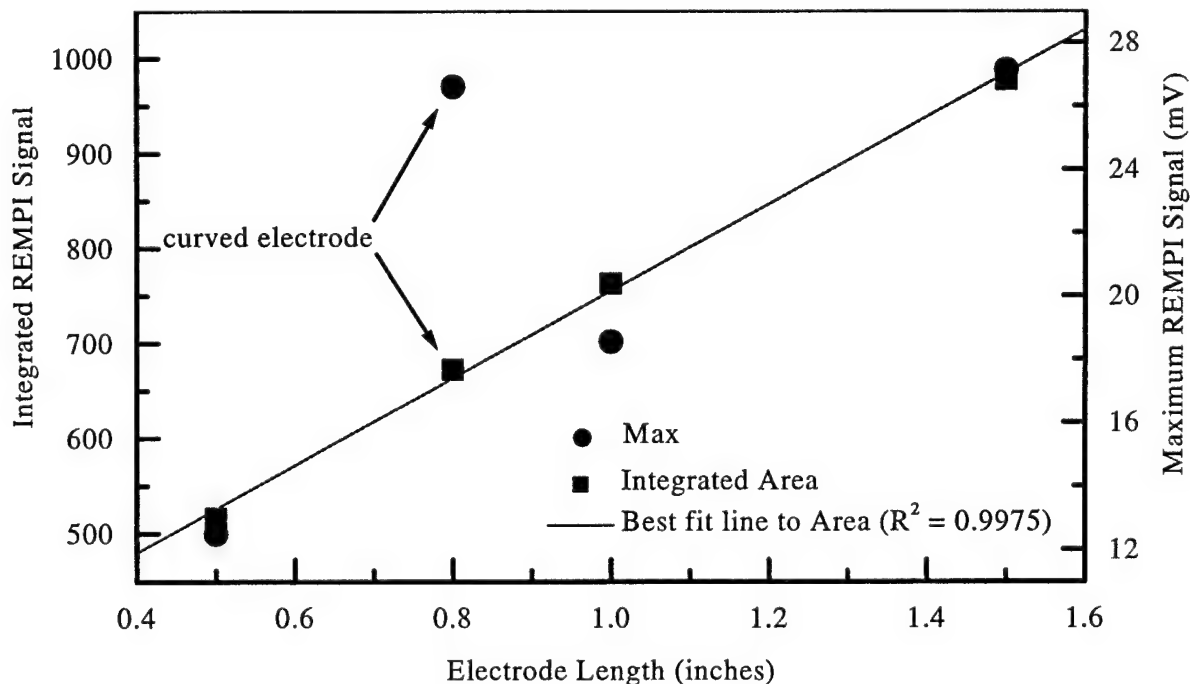


Figure 8. Comparison of waveform maxima and waveform area (data based on Figure 7 waveforms)

## Flow and Pressure Studies

Two variables that are related to the operation of the fuel vapor detector are the flow and pressure of the gas being introduced to the cell. For these tests, a 1 ppm toluene standard was admitted to the cell. For the pressure dependence studies (Figure 9), the flow was constant at 100 mL/min and the pressure within the cell was adjusted by closing a valve on the output side of the cell while increasing the standard gas pressure to maintain the constant flow rate. For the flow rate measurements (Figure 10), the pressure within the cell was assumed constant since there was no restriction on the cell and the standard gas was delivered at minimal pressure (~17 psia). The data shows that the system is quite dependent on the pressure within the cell, but only minimally dependent on flow rate once the rate exceeds 100 mL/min. This led us to design the cell with minimal flow obstruction and utilize a pump that drew vapors in excess of 100 mL/min.

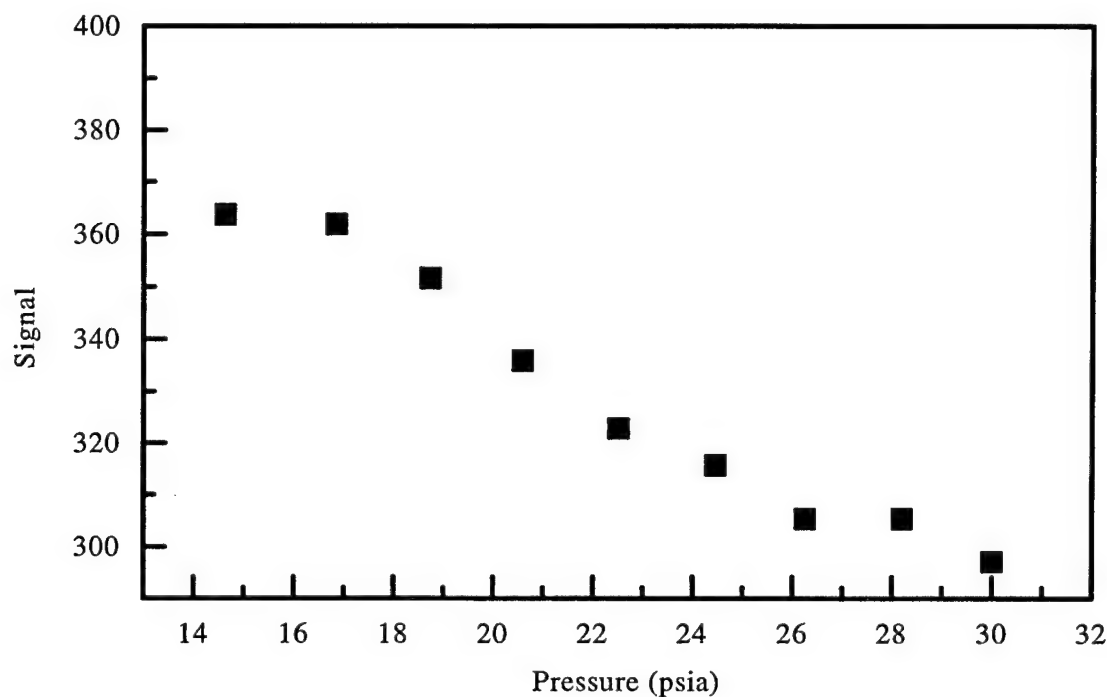


Figure 9. Pressure dependence of the REMPI cell

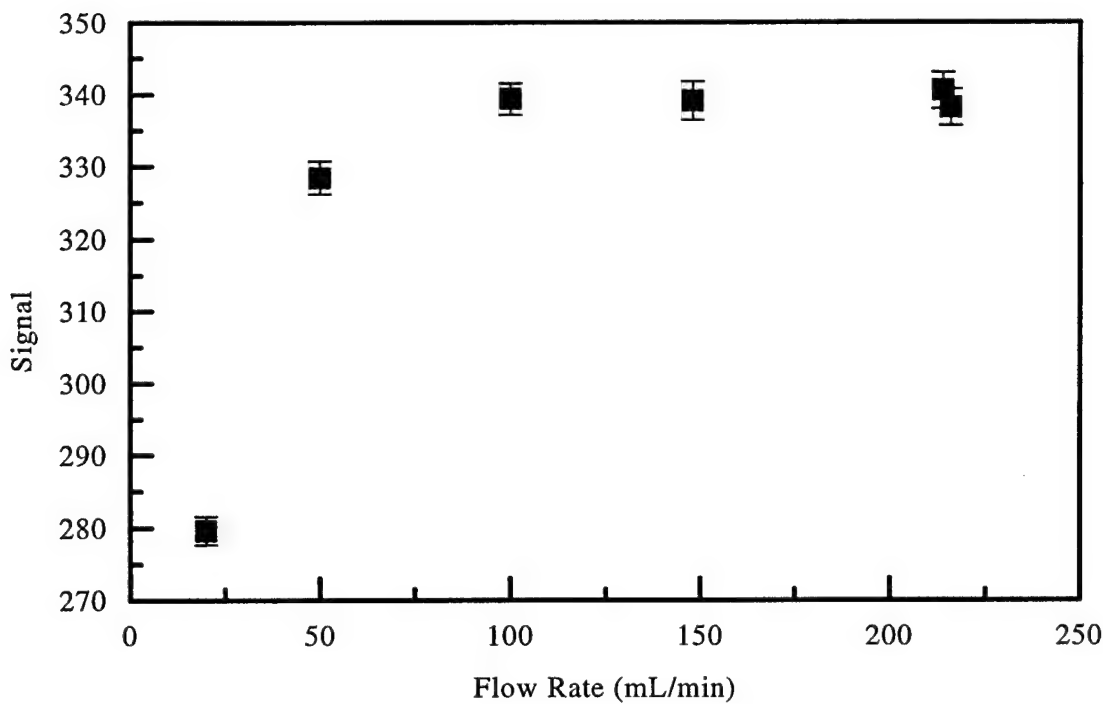


Figure 10. Flow rate dependence of the REMPI cell

#### Electronics Development

Initially a transimpedance amplifier was used to convert the current generated in the REMPI cell to a voltage. An oscilloscope digitized the resultant waveform. This resulted in a cumbersome setup and the amplifiers also seemed to be very short-lived (sometimes only a few days). We identified an alternative to the transimpedance amplifier that we refer to as the integrator (Burr-Brown IVC102). The integrator is essentially a transimpedance amplifier with on-board capacitors to store charge. A microcontroller sets the necessary switches on the integrator to store the charge on the capacitors; the microcontroller also serves as the interface with the control computer. With the integrator we were able to get performance that at least equaled the transimpedance amplifier (see Figure 11) and we never had to replace the integrator. It also simplified the system by eliminating the need for an oscilloscope.

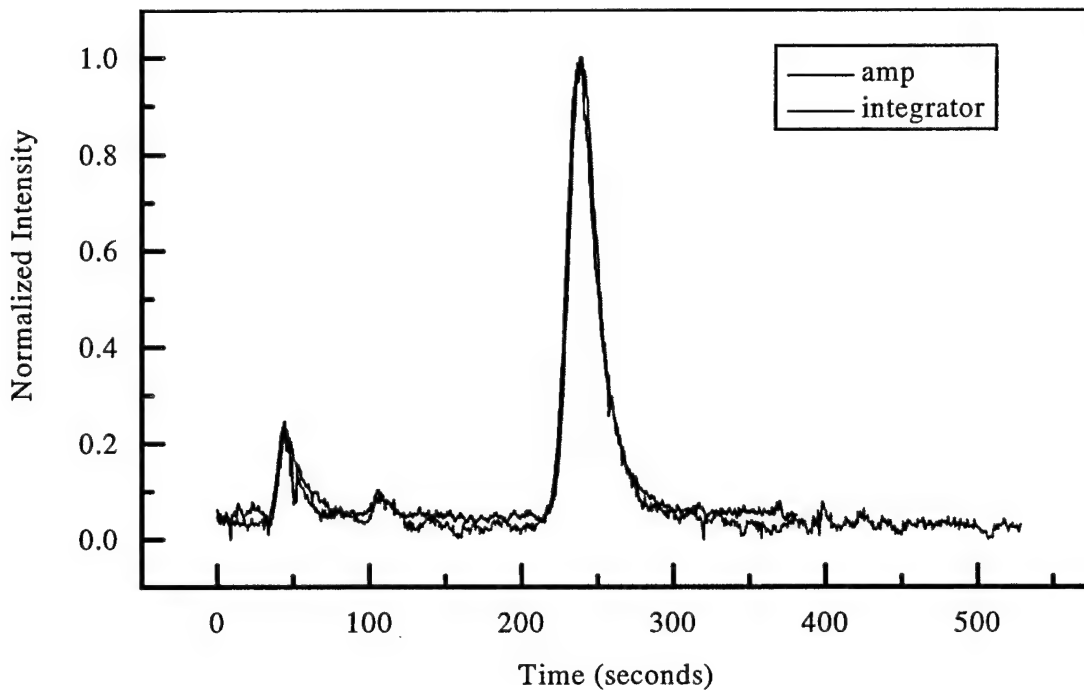


Figure 11. Chromatographic elution of toluene comparing the integrator with the transimpedance amplifier

### Calibration

An important aspect of the system is the ability to conveniently calibrate. We initially investigated using gas cylinders filled with known concentrations of standard gas (1 ppm toluene). However, 1 ppm is more concentrated than we would expect to encounter in real-world applications of the system. Additionally, the cylinders were quite expensive ~\$400 and would provide limited (~300 L) amounts of calibrant. The option settled on was the use of permeation tubes. These are plastic tubes filled with analyte (in our case toluene); the tubes are factory calibrated to emit the analyte at a very constant rate. By drawing clean air over the tube, we were able to obtain a toluene concentration of 10 ppb to serve as a single point calibration. The tubes were modestly priced at ~\$200, and back of the envelope calculations indicated they would last for several decades before they no longer emitted toluene.

### Software and GPS

Software was written in Visual Basic that allowed us to simultaneously monitor integrator response (aromatic concentration in ppb toluene equivalents), relative laser energy, and when necessary global position. The software provided an easy to use interface between man and machine while conveniently displaying the data in real-time.

## Laboratory Studies

### Signal Dependence on Laser Energy

Since 1+1 REMPI is a two-photon process, theory holds that changes in a REMPI signal should vary as the square of the change in photon intensity (for example, doubling the laser intensity should cause the REMPI signal to quadruple, all else being equal). To confirm this dependence, a reference beam measurement and the REMPI signal of a constant concentration of toluene (around 25 ppm) were compared at six different laser intensity settings. Plotting the logarithm of the REMPI signal versus the logarithm of the reference beam measurement gives a slope of about 1.93, which is consistent with the theoretical value of two.

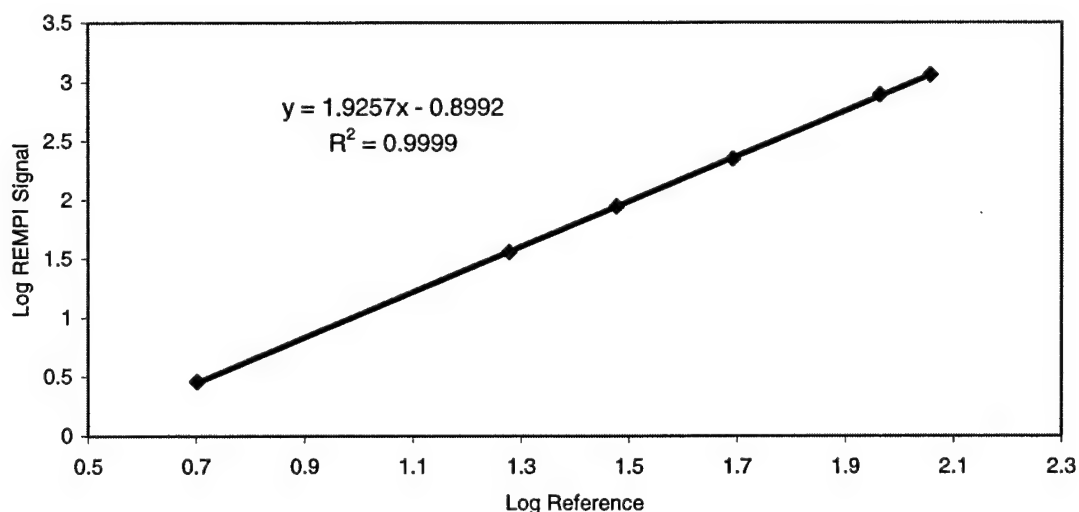


Figure 12. Quadratic dependence of signal on laser energy

### Fiber Optic Delivery of Laser Light

One mode of operation that was explored was delivering light from the laser to the ionization cell via fiber optic. This mode would potentially allow the "detection end" of the system to be smaller, which would have implications with hand-held devices or certain types of probes. Figure 13 shows waveform overlays, where the waveform of smaller intensity was taken prior to sample introduction, and the more intense waveform taken following sample introduction.

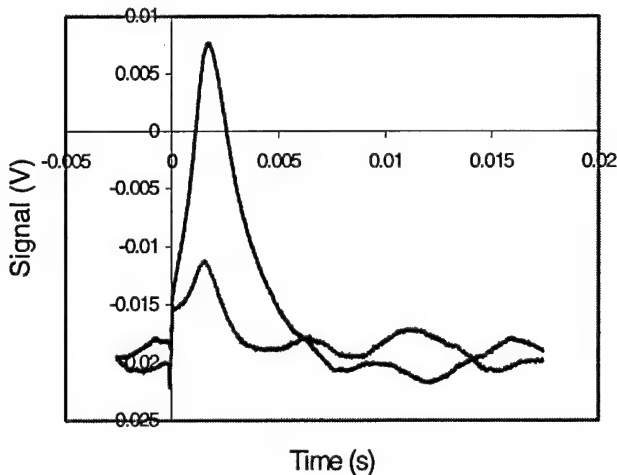


Figure 13. Benzene REMPI signal, 667 ppb (fiber tip between electrodes)

While fiber optic light delivery shows promise, it was abandoned fairly early on in favor of passing the laser beam directly from the laser through the ionization cell. Polarization and other types of fiber damage are problematic, and the fiber's length-dependent attenuation of laser energy hurts the sensitivity that could be achieved by passing the laser beam directly through the cell. In addition, the relative size of other system components and the mode of leak detector operation made the utility of remote light delivery relatively unimportant.

#### Semi-Permeable Membrane Studies

In the real world, sample conditions (temperature, humidity, particulates in the air) will undoubtedly vary substantially on a day-to-day and a point-to-point basis, which challenges the consistency of the detector's response. In addition, it may be desirable to take measurements of liquid samples (BTEX in water), but the analytes must be introduced to the ionization cell as a vapor. To address these issues, we experimented with membrane interface sampling.

For air sampling modes of operation, a "tube within a tube" design was employed. A small diameter, thin-walled piece of silicone tubing (permeable to all of the common VOCs) was arranged concentrically inside a larger stainless steel tube. A pump was used to draw ambient air (the air to be sampled) through the space between the silicone tubing and the stainless steel tube. Analytes pervaporate through the walls of the silicone tube into the interior, where they are entrained in a flow of "clean" air from a compressed gas cylinder and transported to the REMPI cell. To demonstrate this sampling mode, the eluent from a GC was directed through the outer stainless steel tubing at a flow rate of ca. 20 mL/min. The GC injections consisted of 3  $\mu$ L of a solution of toluene in pentane (2.6 ng toluene launched on column), and the flow rate inside the silicone tube membrane was varied. Our expectation that the integrated chromatogram peak area would decrease with increasing flow rate inside the membrane tube (owing to the analyte concentration being reduced at higher flow rates) was confirmed (see Figure 14 and Figure 15). Note that the transfer of analyte across the membrane was unaffected.

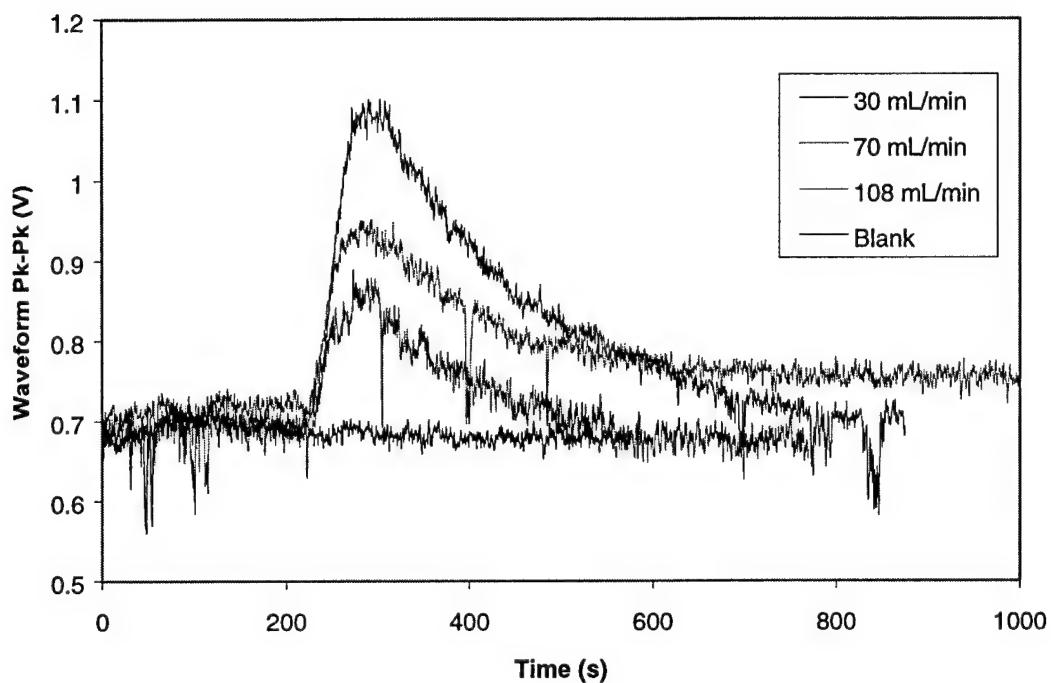


Figure 14. REMPI response as toluene (2.6 ng) was eluted from the GC through the outer stainless steel tube with various airflow rates inside the membrane tube

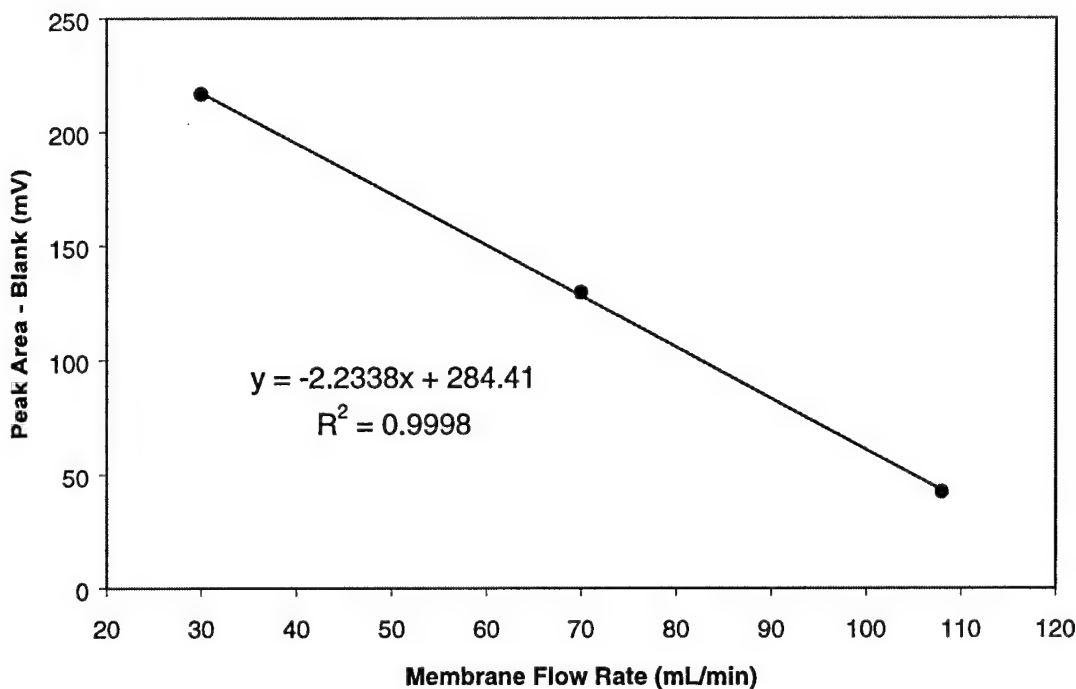


Figure 15. Chromatogram peak areas (2.6 ng toluene injected on column) with varied flow rates inside the membrane tube

To test the feasibility of analyzing water samples for BTEX species via REMPI, a piece of silicone tubing measuring about a foot in length was submerged in a bottle of water, which was periodically "spiked" with known amounts of toluene. A carrier gas, compressed air, swept analytes permeating through the silicone tubing into the REMPI cell. Figure 16 and Figure 17 show the raw data and a calibration curve, respectively. The data are linear over at least three orders-of-magnitude and the limit of detection is in the low ppb range ( $\mu\text{g/L}$ ). Addition of a ballistically heated trap between the silicone rubber tubing and the REMPI cell could further improve the limits of detection.

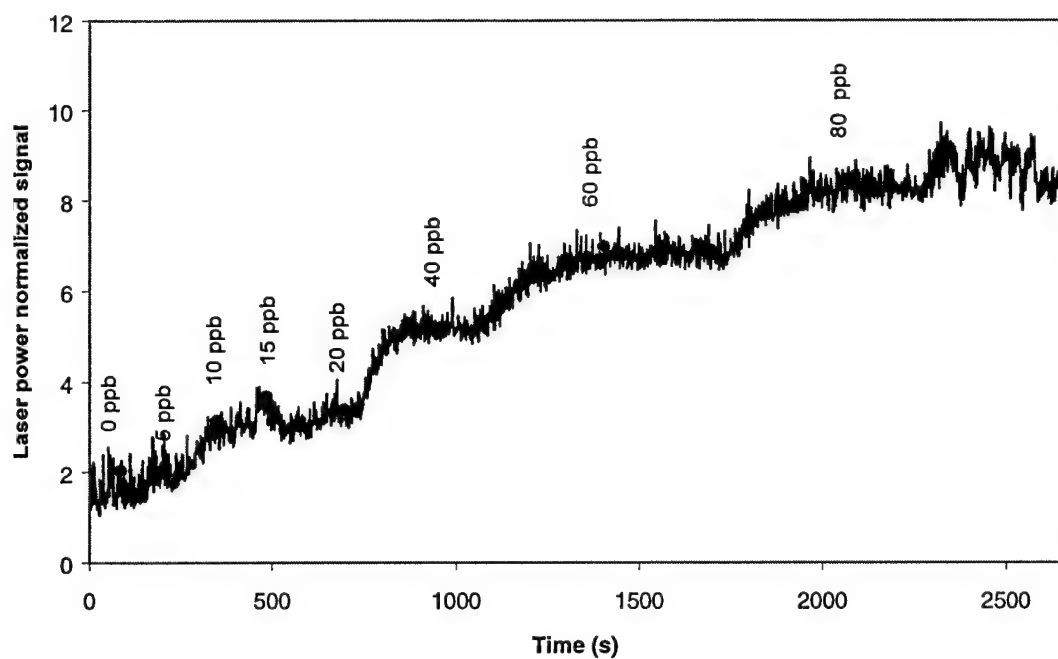


Figure 16. Incremental additions of toluene to water – sampling with silicone tube membrane (air flow = 25 mL/min)

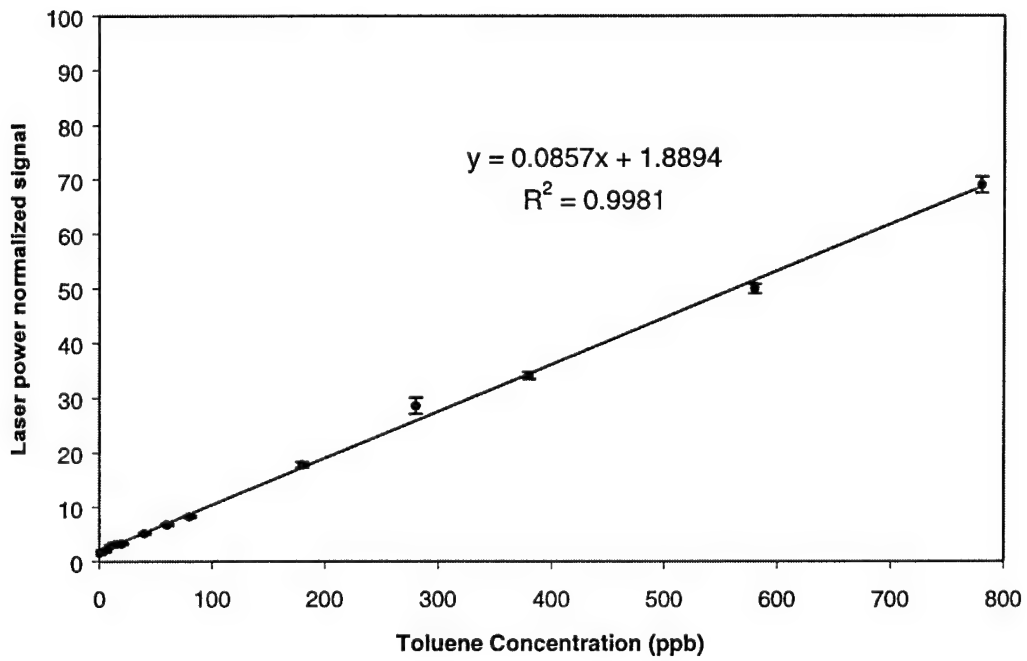


Figure 17. Calibration curve of toluene in water – sampling with silicone tube membrane

### Sorbent Interface Studies

A Tenax trap, which can be rapidly heated, was used to pre-concentrate toluene samples to achieve larger signals with the leak detector. Clean air, which had been passed through a carbon filter, was used as a blank, and signals were recorded for trap loading times of 0, 30, 60, 100, and 200 seconds. A toluene permeation tube (emission rate = 105 ng/min, air flow rate = 410 mL/min, concentration = 62 ppbv) was then put in-line with the air flow, and signals were recorded for the same trap load times. The differences between the toluene signals and the blanks are plotted vs. trap loading time in Figure 18.

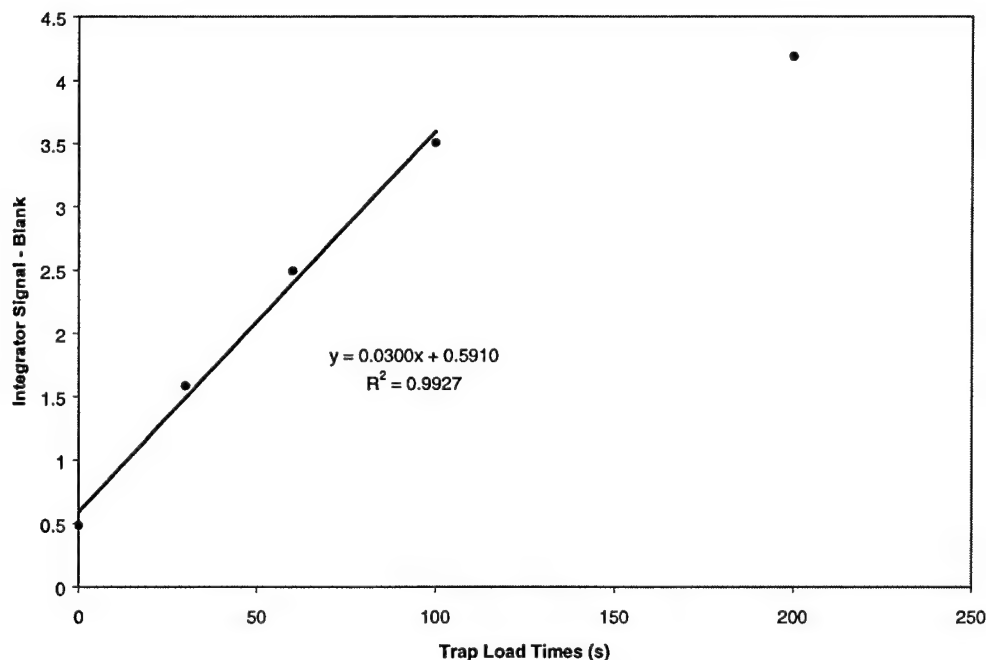


Figure 18. Toluene signals as a result of pre-concentration with a Tenax trap

We can see from the figure that the signal increases linearly with trap loading time, up to around 100 seconds. As the trap becomes "full," it can no longer pre-concentrate all of the inflowing toluene, and the trend falls out of linearity.

### Dust Elimination

During several of our field studies, large amounts of dust accumulated in the REMPI cell. If the dust had BTEX adsorbed onto it, a resulting "carryover" signal was seen. Furthermore, if the dust reached the pump, its lifetime was greatly reduced.

To eliminate these issues, several filtering systems were tested using a dust generator (Figure 19) to find an efficient means of blocking dust intrusion. The filtering methods tested included a single layer of non-woven cloth, multiple layers of non-woven cloth, Gore-Tex coated cloth, and

a metal frit. The most efficient filtering system found was a metal frit. This filter was employed during the Tinker Air Force Base field demonstration.

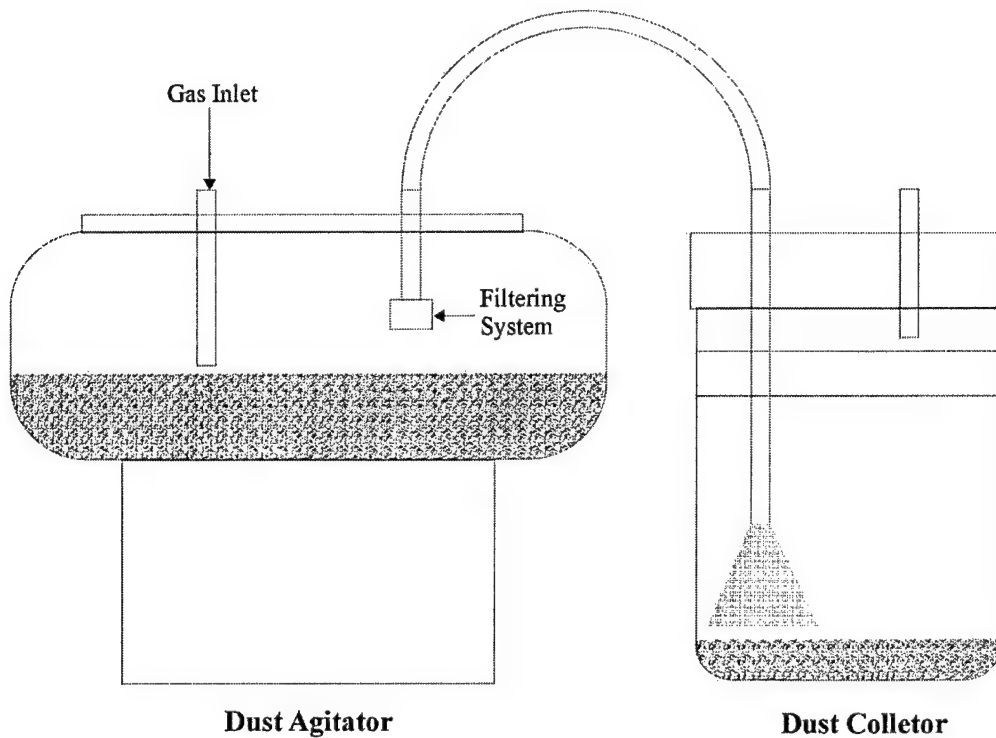


Figure 19. Dust generator used to test different filtering systems

#### Responsivity of the Detector

Figure 20 shows a waveform captured with the use of a transimpedance amplifier for a low concentration of toluene. A toluene permeation tube was used to set the concentration. Figure 21 shows a low-concentration calibration curve for toluene, clearly demonstrating the ability of the leak detector to detect low-ppb levels.

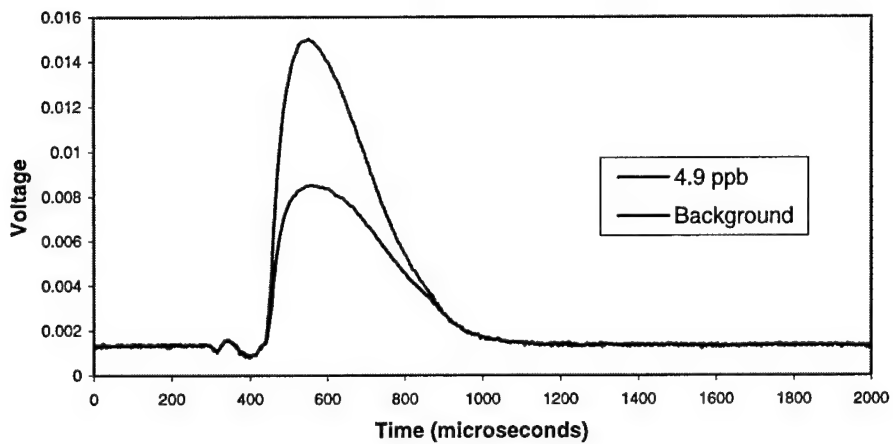


Figure 20. Response waveforms for 4.9 ppb toluene and background signal

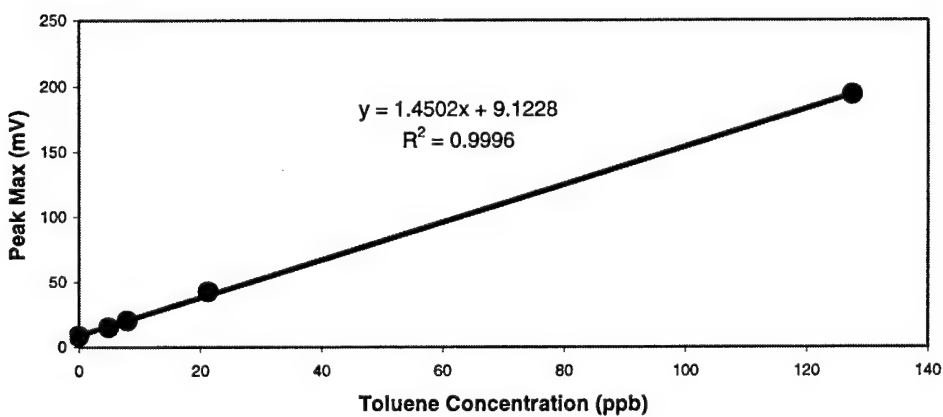


Figure 21. Low concentration calibration curve for toluene

Figure 22 shows a toluene calibration curve at a higher concentration range, demonstrating continued linearity of response through a range four orders of magnitude away from the low concentration levels shown in Figure 21. The raw signal in Figure 22 was divided by the square of the laser pulse energy (quadratic signal dependence) to correct for the slight differences in laser pulse energy.

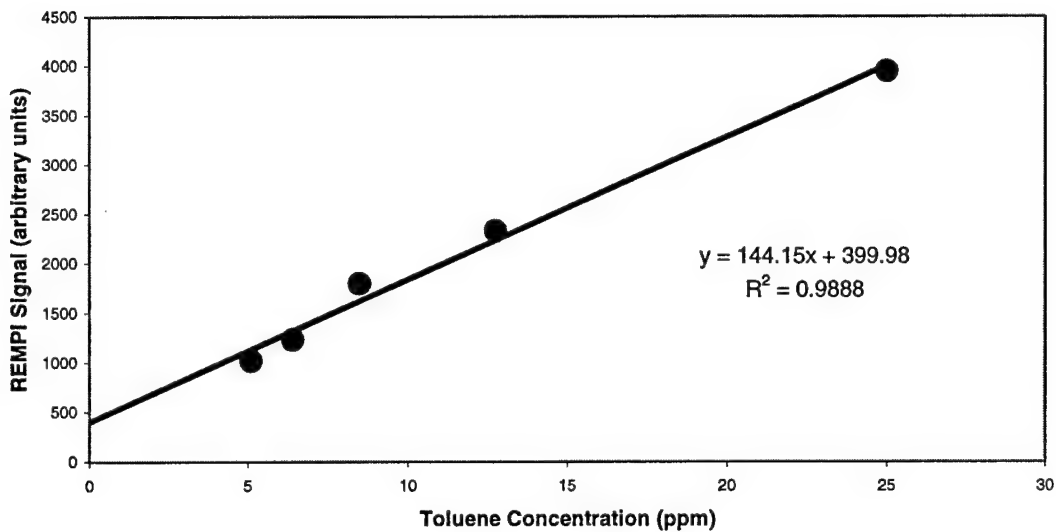


Figure 22. Higher concentration calibration curve for toluene

In another style of experiment, the effluent from a GC was directed into the leak detector ionization cell and the responses from a series of injections of dilute toluene solutions were recorded. The data are shown in Figure 23.

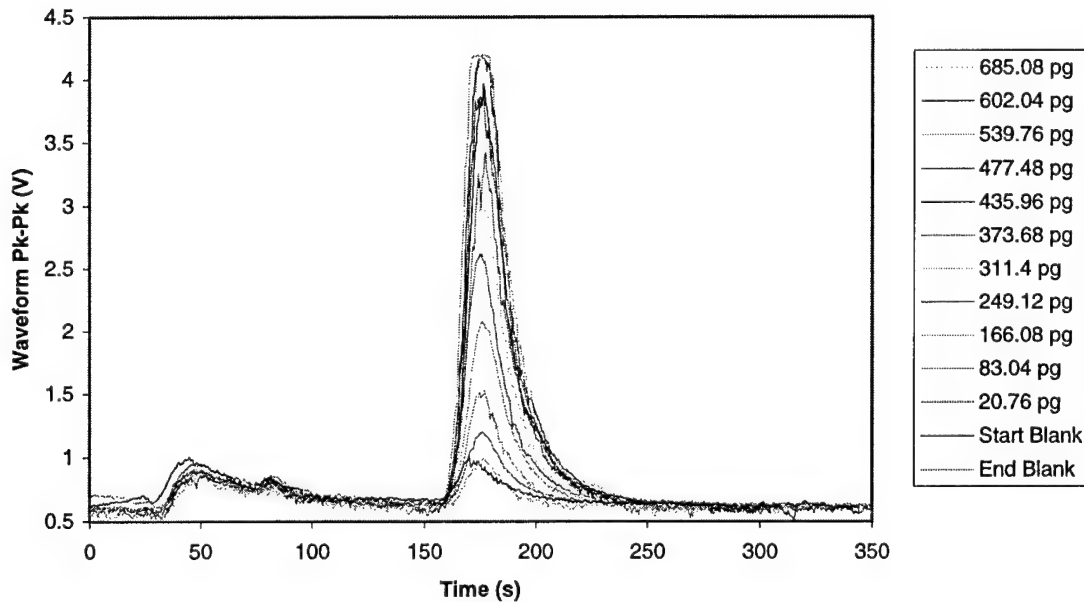


Figure 23. Chromatograms of toluene eluted from a GC column

Eventually, the use of a transimpedance amplifier was abandoned in favor of a current integrator, for reasons discussed previously (see System Development) in this report. Figure 24 shows an initial data set taken with the current integrator. The data in Figure 25 was taken at a more mature stage of integrator development, and indicates a detection limit for toluene of less than 2 ppb.

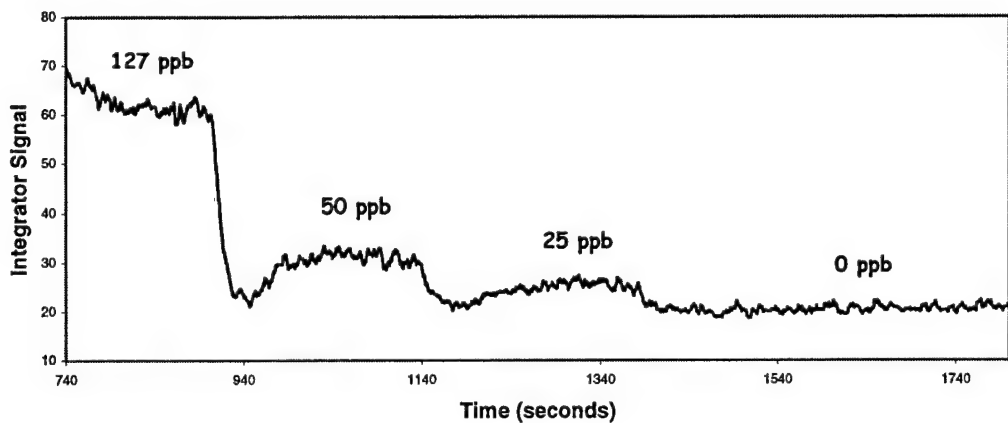


Figure 24. Initial current integrator response for various toluene concentrations

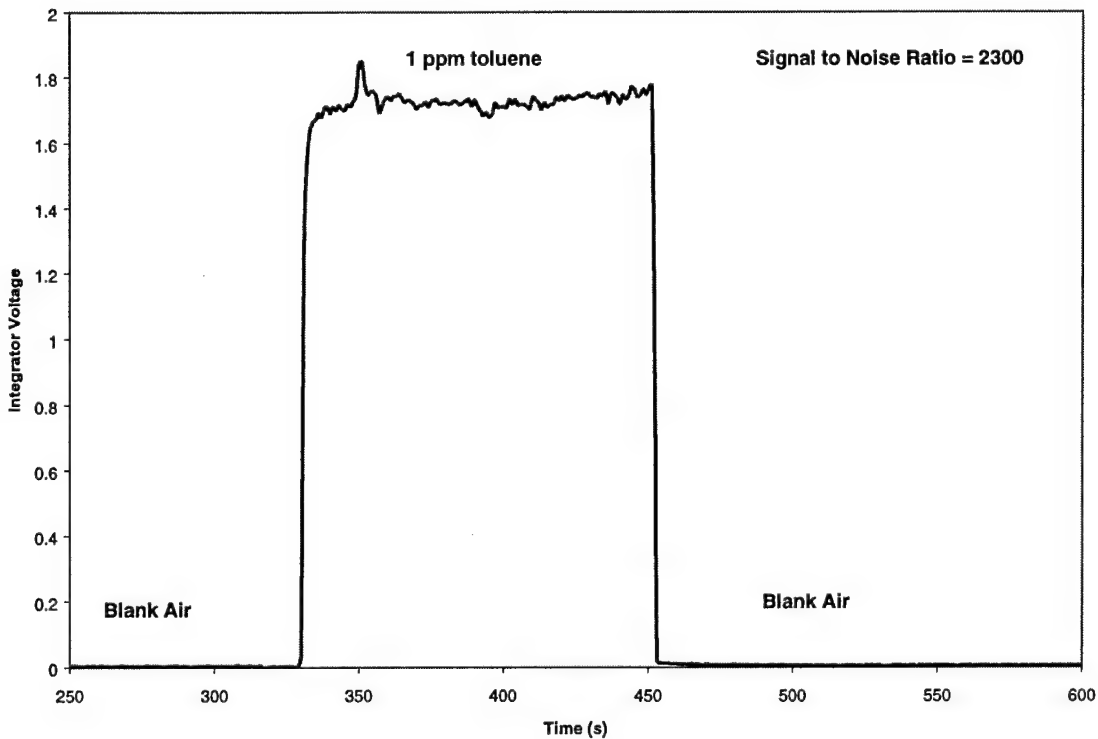


Figure 25. Current integrator response with blank air and 1 ppm toluene standard gas  
The signal to noise ratio of 2300 for 1 ppm toluene implies a limit of detection of 1.3 ppb.

The detection limit estimates shown Table 1 in were calculated by extrapolating the data from an experiment where small volumes of saturated headspace were diluted in a large volume vessel and introduced to the leak detector. The data is presented in two ways to reflect different ways one could think about detection. The first column represents detection limits as a fraction of saturated headspace that is quantifiable, or by what factor, saturated headspace could be diluted and still be detectable. This number doesn't directly consider the concentration of analyte in saturated headspace, but rather considers saturated headspace as the target to be detected, which is useful when thinking about how well a large spill could be found in an outdoor environment. The second column simply lists the analytes' vapor pressure, or the concentration of the analyte in saturated headspace. The third column, which is the product of columns 1 and 2, then gives the limits of detection of the analytes themselves.

To illustrate why it's useful to consider both of these detection limit values, consider the data pertaining to gasoline and diesel #2. As seen in column 3, the leak detector is much more sensitive to pure diesel #2 vapor than to pure gasoline vapor, but because the vapor pressure of diesel #2 is more than 400 times lower than that of gasoline, it would be much more difficult to detect and locate a diesel #2 spill than a gasoline spill in an outdoor or subsurface situation (column 1).

Table 1. Limits of detection for select BTEX and fuel components

	<b>LOD: Fraction of Saturated Headspace in Sample (ppmv)</b>	<b>Fraction of Analyte in Saturated Headspace (vapor pressure in atm, 25 °C)</b>	<b>LOD: Fraction of Analyte in Sample (ppbv)</b>
Toluene	0.0748	0.0376	2.8138
Benzene	0.3248	0.1285	41.7410
Gasoline	0.4403	> 0.53*	233.3598
Diesel #2	18.3923	< 0.00132*	24.2778
Kerosene	20.3279	< 0.00658*	133.7573
JP-4	2.2721	0.1197**	271.9667
JP-8	9.9184	< 0.00658*	65.2629

\*Values taken from Exxon/Mobil's data sheets

\*\*Values taken from Langley AFB estimates

(<https://denix.cucer.army.mil/denix/Public/Library/Remedy/Langley/langly02.html>)

#### Selectivity Towards Aromatic Hydrocarbons

The selectivity of the leak detector towards aromatic hydrocarbons was evaluated by comparing the response to that of a universal detector, a photoionization detector (PID), for mixtures of aromatic and aliphatic hydrocarbons. The individual components were temporally separated with the use of a GC, and the two detectors were hooked up in series at the end of the column for simultaneous data collection. Figure 26 and Figure 27 show chromatograms for two types of jet fuel, JP-4 and JP-8. Note that only a few peaks are seen with the leak detector because it responds only to the aromatic molecules in the sample.

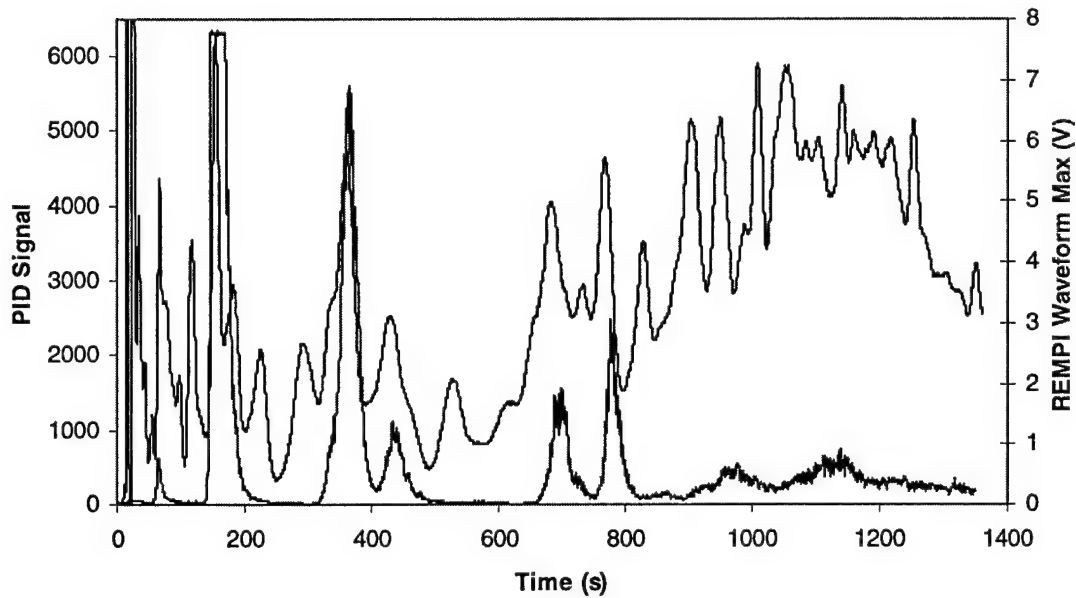


Figure 26. Leak Detector and PID response to JP-4 injected on column

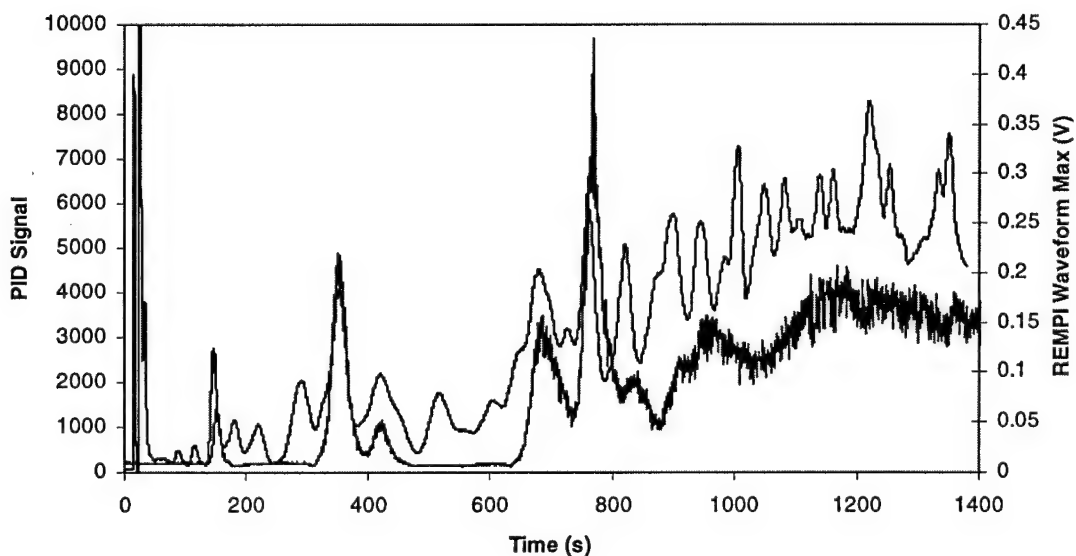


Figure 27. Leak Detector and PID response to JP-8 injected on column

Figure 28 shows a chromatogram taken in the same fashion for a 1% gasoline solution in hexanes. The GC parameters were somewhat different than before, so component retention times aren't the same as seen in the jet fuel chromatograms. The elution order of the BTEX

species was determined by injecting dilute standards of individual compounds; a chromatogram taken for a BTEX mixture in hexanes is shown in Figure 29.

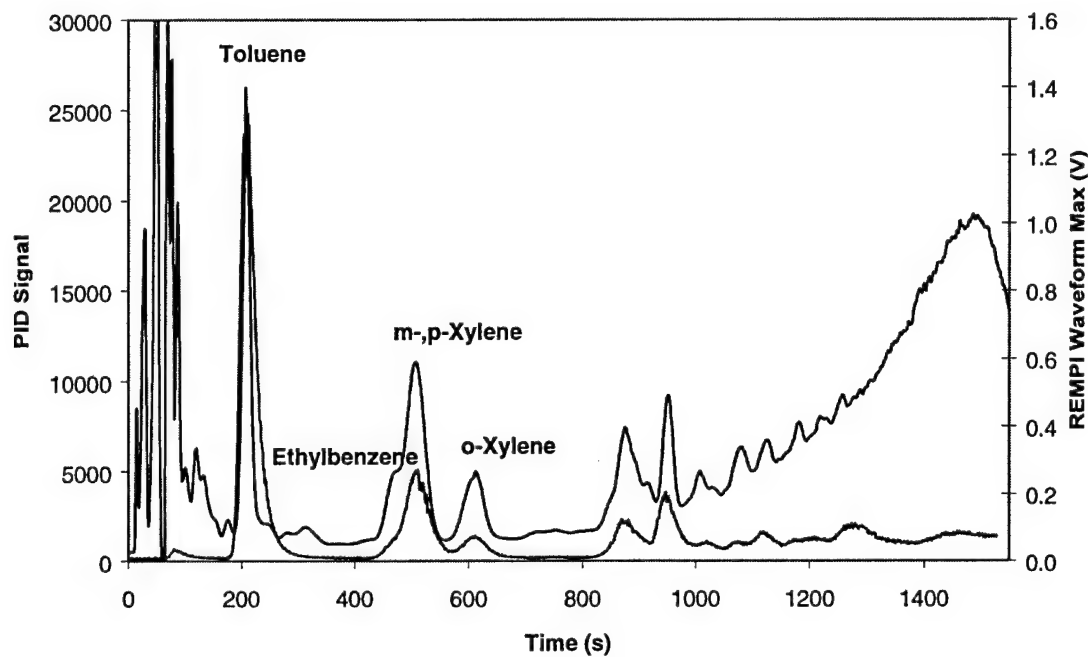


Figure 28. Leak detector and PID response to gasoline (in hexanes) injected on column

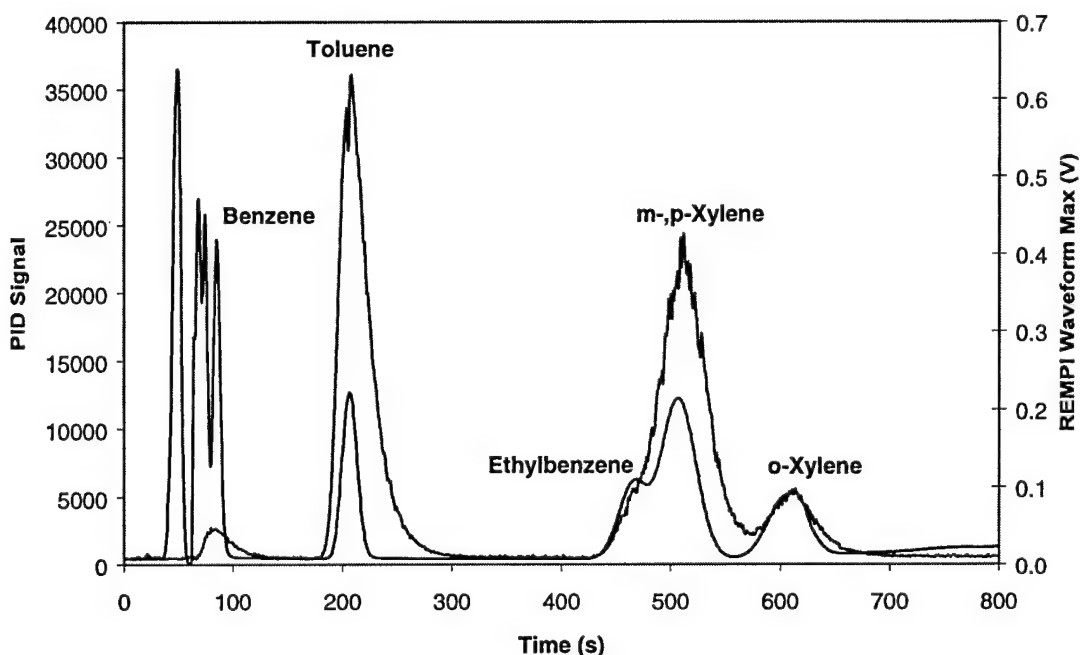


Figure 29. Leak detector and PID response to a BTEX mixture in hexanes

## Field Studies

### Pipeline Leak Detection in Western North Dakota

In October 2001, we arranged a trip to Tioga, North Dakota, where Amerada Hess has many buried pipelines carrying either crude oil or natural gas condensate (wet gas). They identified four areas for us to sample. One was a site where approximately 2 years ago there had been a leak in a wet gas pipeline. Two other areas included a wet gas leak that had been repaired 4 months ago and an active wet gas leak. The fourth site was a recently (~3 days) repaired crude oil leak. Conversations with their field workers revealed how leaks are currently detected, repaired and remediated. With the low value products associated with these leaks, the detection schemes are quite crude. A plane is flown over the pipeline to look for dead or distressed vegetation. They excavate the site and patch the leak typically with a rubber membrane under a stainless steel band. The dirt that is excavated from the site is spread out on the ground and treated with fertilizer to encourage bacterial growth. After a few days, the dirt is returned to the excavation area.

At the actively leaking wet gas site, five east-west transects were performed across the site. The pipeline ran (from northwest to southeast) through a recently harvested wheat field and the wheat stubble above the leak was slightly discolored relative to the rest of the field. Data collected at this site is shown in Figure 30. The northernmost transect (transect #1) was about 50 feet north of the discolored wheat. All transects were approximately 25 feet apart and transects were created by taking a discreet data point at ground surface every 5 - 6 feet along the transect for

approximately 100 feet. The actual leak was approximately 25 feet south of the southernmost transect (transect #5). Typical with wet gas leaks there was a significant amount of hydrogen sulfide present and for safety reasons, the field workers would not allow us to probe directly over the leak.

At the other two wet gas sites, (the 2 year old and the 4 month old) there was no change in signal relative to background areas. This is a substantial result since it indicates that once properly repaired and remediated the leak detector will not give false positives at sites that have repaired leaks.

The final site investigated was one where there had been a crude oil leak. This site had been repaired and backfilled with the treated soil. Data from the site is shown in Figure 2. The pipeline ran east-west across a plowed wheat field. There were three north-south transects (approximately 25 feet apart) across the heart of the excavated area. Transect #1 is the easternmost transect and gave the strongest signal. Transect #2 was in the middle of the excavated area, but because of a data collection error, we were not obtaining GPS data, the data appears to be a single point. As the data was being collected however, it was apparent that it was consistent with Transect #1. Transect #3 extends further to the north (about 100 feet) than the other transects. This was done to collect background data from an area away from the pipeline.

At this site we also explored sampling options; the data is shown in Figure 32. At the other sites, a sampling pan was placed on the ground and vapors were drawn into the REMPI cell *via* a mechanical pump. This process was fairly slow and required about 30 seconds at each point for the system to equilibrate. To speed up the process we attached the sampling tube to the cart such that it dragged on the ground and slowly walked along the pipeline (east-west). We did this for two trials (drag #1 and drag #2 in Figure 32). The signals obtained (the left axis in Figure 32) from the dragging were very small relative to those obtained on the north-south transects, but the transects produced signal profiles that were consistent with intensities observed in the north-south transects. The final approach involved using a stainless steel rod to create a  $\frac{1}{2}$ " hole in the ground about 6" deep and then inserting the sampling hose into the hole. This method was used on the same path as the drag method and gave a similar profile albeit with substantially higher signals (holepunch in Figure 32). This demonstrated that it is very important to break the ground surface to obtain the highest signals.

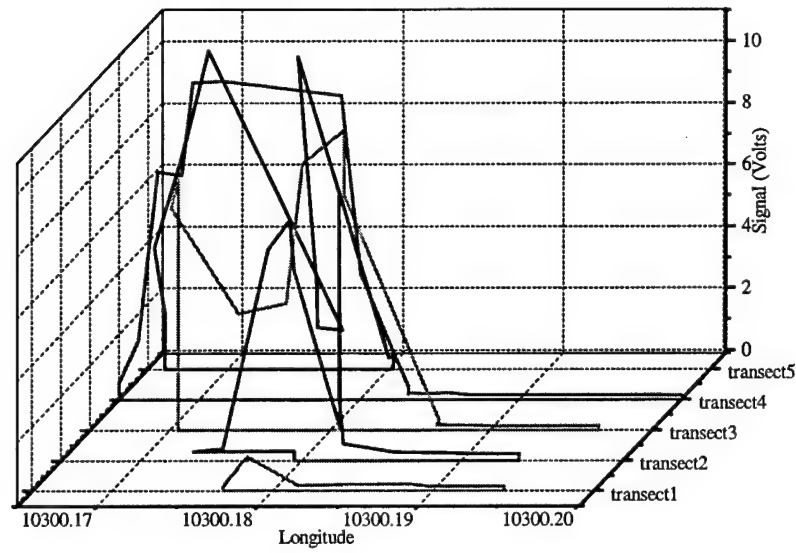


Figure 30. Data collected at a leaking wet gas site

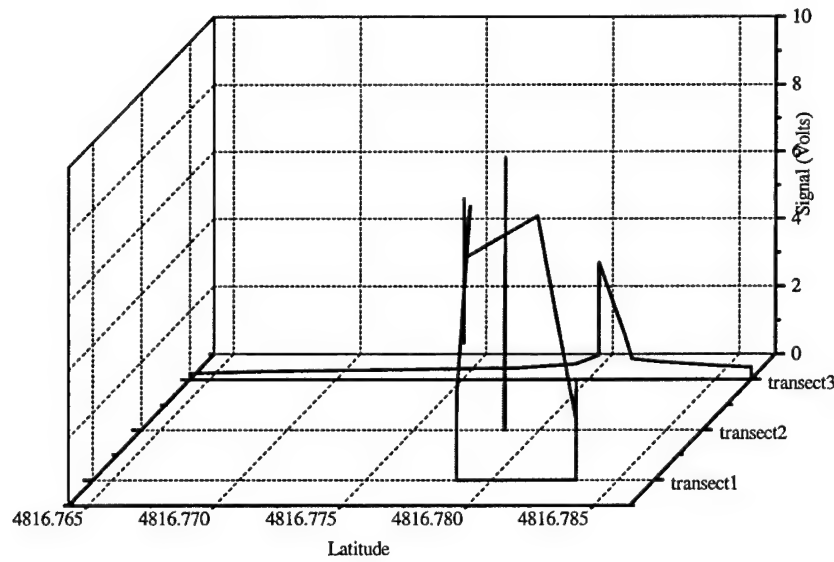


Figure 31. Data collected at a repaired crude oil leak site (north-south transects)

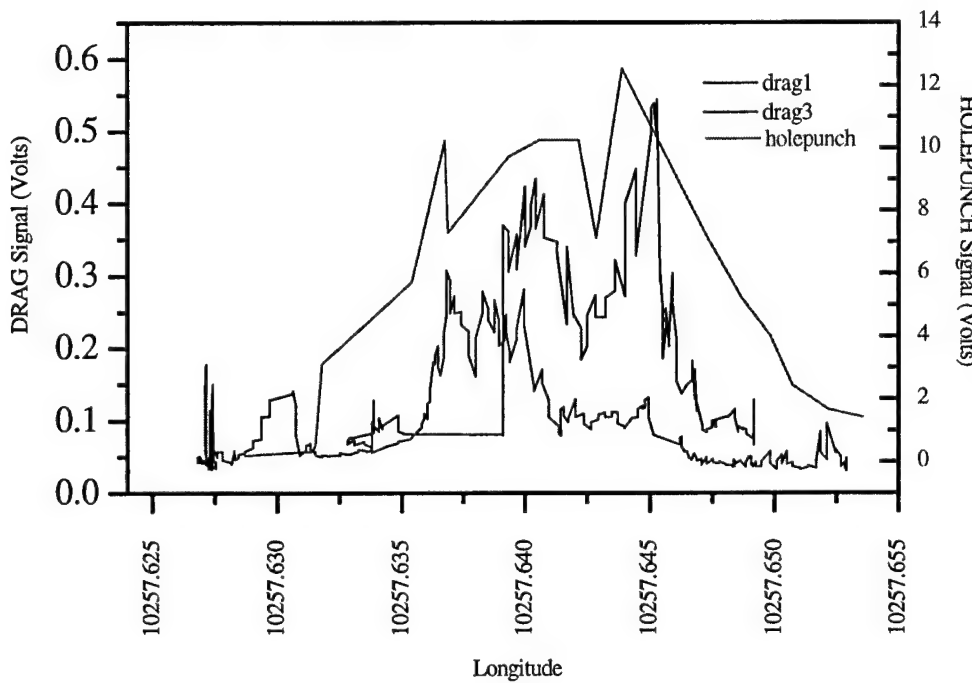


Figure 32. Different sampling strategies used at crude oil site

#### Field Testing at Offutt Air Force Base

The mobile leak detector system was deployed on November 19 and 20, 2001 for field-testing at Offutt Air Force Base in Omaha, Nebraska. Several sites were chosen for evaluation based on past or suspected fuel spills, however, none of the sites chosen were known to be currently leaking. Unfortunately, sampling problems severely limited the effectiveness of the studies. The most critical of these issues was contaminated soil that would linger in the sampling probe, which would then "carryover" signal to each subsequent sampling point. We developed an inline filter system to remedy this problem.

An aboveground fuel pipeline with multiple joints was successfully evaluated. As shown in Figure 33, a particularly strong signal (near a leaking valve) was detected by both the leak detector and the handheld MiniRAE 2000 PID (data collected simultaneously). Dr. Don Campbell (EPA) was also on-site with an LEL detector, which was not able to detect this leak. There were a number of other points where the leak detector picked up faint signals, while the PID and LEL were unresponsive.

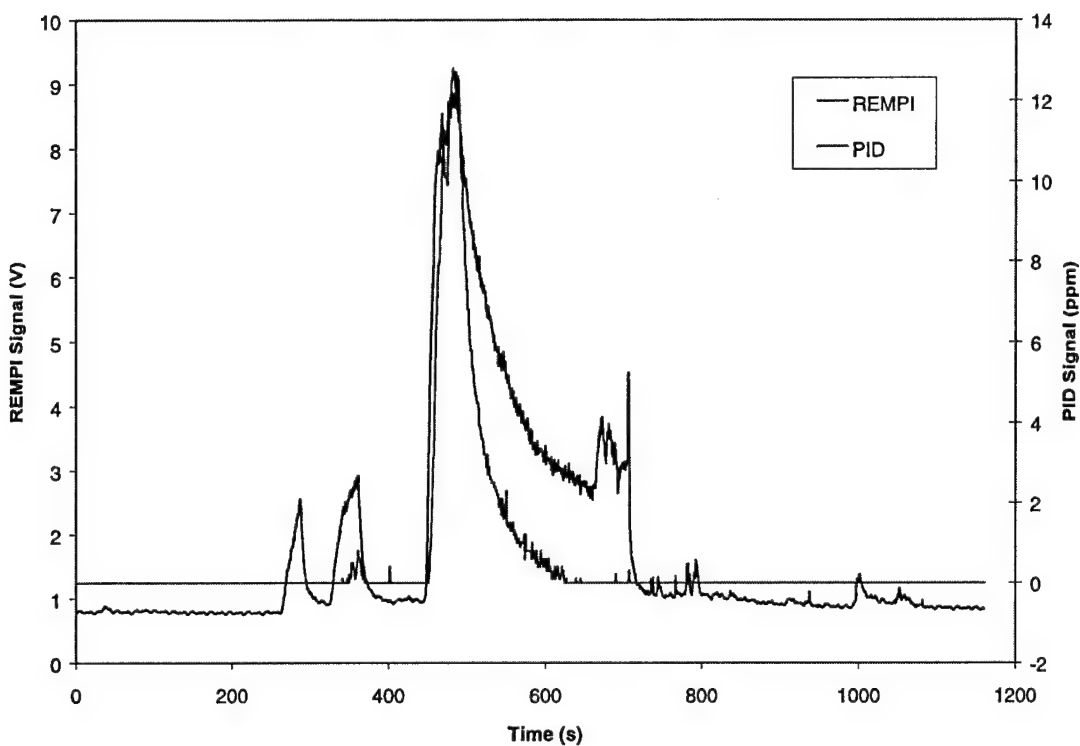


Figure 33. Leak detector and PID signals from the evaluation of an above-ground fuel pipeline with several joints and valves

#### Field Testing near Lamesa Texas.

Soil gas was sampled at 15 locations near Lamesa Texas to compare the performance of the fuel vapor detector with an established methodology for field analysis of soil gas. New Paradigm Exploration, an oil exploration company that utilizes soil gas analysis as an indicator for potential drilling locations, had previously sampled the sites.

Samples were collected by auguring a  $\frac{3}{4}$ " hole in the ground to a depth of approximately 18 inches. The hole was sealed from the atmosphere by inflating a packer. Twenty milliliters of soil gas was withdrawn from the hole and expelled before a one hundred milliliter sample was collected. The sample was injected into a field gas chromatograph that operates at ambient temperature and uses a surface acoustic wave detector. The GC was calibrated by injecting 100 mL of a calibration gas that consists of 200 ppb each of benzene, toluene, ethylbenzene, and xylene(s). A microprocessor in the GC quantifies the chromatographic peaks and assigns retention times. The results are summarized in Table 2.

Table 2. Summary of the results obtained by New Paradigm Explorations for benzene, toluene, ethylbenzene (e-benzene) and total xylenes in parts per billion (ppb). Sample location is in the left column and analyte is in top column.

	benzene	toluene	e-benzene	xylenes
Og01	29	38	0	0
Og02	26	28	21	0
Og03	22	36	24	0
Og04	76	3	26	0
Og05	24	28	23	0
Og06	0	64	19	0
Og78	16	22	26	0
Og79	16	33	24	0
Og67	19	20	23	0
Og66	107	32	27	0
Og65	26	45	34	0
Og64	0	35	28	0
Og63	0	38	28	0
Welsh 01	54	32	23	0
Welsh 02	28	27	24	0

The inlet of the fuel vapor detector was modified to contain a Luer-lock hypodermic syringe needle to conveniently interface with the sample syringe. The RAE Systems miniRAE 2000 photoionization detector (PID) served both as a pump to draw the sample from the syringe and as a confirmatory measurement technique. At no time did the PID register a reading above 0.0 ppm (its lowest reading) from a borehole sample. During the initial run, the PID was calibrated with 100 ppm isobutylene calibration gas.

### Calibration Procedure

To calibrate the fuel vapor detector, the 100 mL sample syringe was charged with 10 mL of 1 ppmv toluene in air standard and diluted with ambient air to 100 mL to prepare a calibration standard that is 100 ppbv. This standard was then injected into the fuel vapor detector in the same manner as borehole samples.

### Soil Gas Analysis with Fuel Vapor Detector

At each site, a sample was collected below ground surface (bgs), at most sites another sample was collected at 3 inches above ground and 2 feet above ground. Samples were also collected from 8 feet in the air to represent background samples. Additionally, some samples were collected by drawing the air in through a RAESystems carbon filter to remove any VOC contaminants. The data are summarized in Table 3. At station Og03, two boreholes (approximately 3 feet apart) were drilled and a 100 mL sample was collected from each for injection into the fuel vapor detector. At stations Og04, Og05, and Og06 two bore holes were

drilled and the fuel vapor detector was collected from the second borehole. At all other locations samples for the GC and fuel vapor detector were collected from the same bore hole. The bore holes were collapsed before samples were collected above ground surface.

Table 3. Summary of analysis of samples (total aromatics in ppb toluene) collected near Lamesa Texas. The left column is sample location (Og = Ogallaga) and the top row is sample type: bgs = below ground surface; 3" = 3" above ground; 2ft = 2 feet above ground; 8ft = 8 feet above ground; 8ftC = 8 feet above ground with carbon trap; 100ppb = 10:1 dilution of 1 ppmv toluene in air.

	bgs	3"	2ft	8ft	8ftC	100ppb
Og01	23.3					
Og02	14.1 ± 3.5	14.7 ± 6.1	11.2 ± 7.3	1.3 ± 5.5		99.3 ± 8
Og03	55.2 ± 8 (30.3 ± 11.2)	8.9 ± 13.6	22.5 ± 8.9	19.2 ± 15.2		
Og04	43.1 ± 6.6	33.1 ± 14.5	32.7 ± 10.4	37 ± 11(25.1 ± 12.8)	19.6 ± 7.9	
Og05	60.88 ± 14.2	13.2 ± 10.4	22.2 ± 7.5	22.2 ± 5.6		97.4 ± 13.3
Og06	18.94 ± 8	17.4 ± 6.4	17.7 ± 13.7	16.8 ± 9.9	26.3 ± 14.4	99.3 ± 8.3
Og78	22.6 ± 13.3			22.6 ± 20.6		98 ± 8.7
Og79	25.5 ± 11.7	10.7 ± 11.4		8 ± 8.7		
Og67	35.9 ± 14.8	25.2 ± 11.4		29.1 ± 15.9		
Og66	49.9 ± 10.8	13.9 ± 11.3	15.2 ± 13.1	24.4 ± 13.2	16.2 ± 9.2	
Og65	39.2 ± 14.2	17 ± 10.7	10.5 ± 6.9	23.6 ± 14.4		
Og64	40.3 ± 17.3	18.6 ± 12.6	16.4 ± 21.0	16.1 ± 11		
Og63	24 ± 16.2	14.2 ± 10.5	16.1 ± 12.0	12.8 ± 9.7		99.8 ± 8.2
Welsh 01	35.1 ± 11.5	10.6 ± 4.7	13.6 ± 5.9	17.8 ± 12.6	18.2 ± 8.2	
Welsh 02	24 ± 5.7			11.4 ± 7.1		

The most perplexing observation is the high signal obtained when air was drawn through the carbon trap. We have previously demonstrated that using a carbon trap effectively cleans the air of detectable species; this leads us to believe that there may be contamination of the sample syringe; therefore to obtain meaningful values from the other samples, it is necessary to subtract approximately 20 ppb due to this unexplained background.

It was hoped that comparison of the signal obtained from the fuel vapor detector would scale with signals obtained from the GC, however, there appears to be no correlation upon inspection of the data in Tables 1 and 2. One potential reason for the lack of correlation is the presence of a background interferent. After completion of the study, it was learned that some of the cotton fields in the area may have been treated with the pesticide Trifluralin ( $\alpha,\alpha,\alpha$ -trifluoro-2,6-dinitro-N,N-dipropyl-p-toluidin). The chemical structure (Figure 34) is:

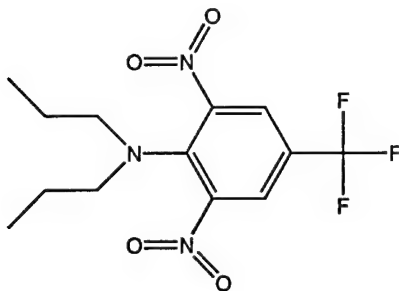


Figure 34. Chemical structure of Trifluralin

While we have never investigated this compound by laser ionization, the aromatic ring indicates that it is very likely that this molecule could be ionized by the fourth harmonic of the Nd:KGW laser. All samples collected had minuscule amounts of aromatics present (tens of ppb) therefore the presence of even a trace of Trifluralin could significantly skew the results.

#### Field Testing at Tinker Air Force Base

The mobile fuel vapor detector system was deployed on March 26 and 27, 2002 for field-testing at Tinker Air Force Base in Oklahoma City, Oklahoma. Two buildings (buildings 976 and 230) were chosen for evaluation based on the likelihood of fuel vapors (building 976) and on-going air quality issues (building 230). The following sections describe the calibration procedure and results obtained at each building.

#### Calibration Procedure

The fuel vapor detector system was calibrated prior to use in both buildings. The MiniRAE 2000 PID — which serves dual functions as the system's pump and second detector— was calibrated using a 100-ppm isobutylene calibration gas. All concentrations reported with the PID are referenced to this calibration with units of ppm isobutylene equivalents.

The calibration for the fuel vapor detector consists of routing outside air through a carbon scrubber to remove any residual BTEX vapors. Next, a toluene permeation tube (emission rate = 105 ng/min, air flow rate = 540 mL/min, concentration = 47.25 ppbv) is put in-line between the carbon scrubber and the detector. The resulting signal is used to calculate a conversion from volts to concentration with units of ppb (toluene equivalents). The units used for the fuel vapor detector are analogous to the units used for the PID.

#### Building 976

The fuel vapor detector was deployed in building 976 (Fuel Systems Repair). The measurements taken in this building were used to assess whether our system was operating properly. Since no aircraft were actively being serviced, a fuel bowser was brought inside the building to supply fuel vapors. A diagram of the locations where measurements were taken inside the building with the fuel vapor detector is shown in Figure 35. The resulting logs generated at each location are shown in Figure 36.

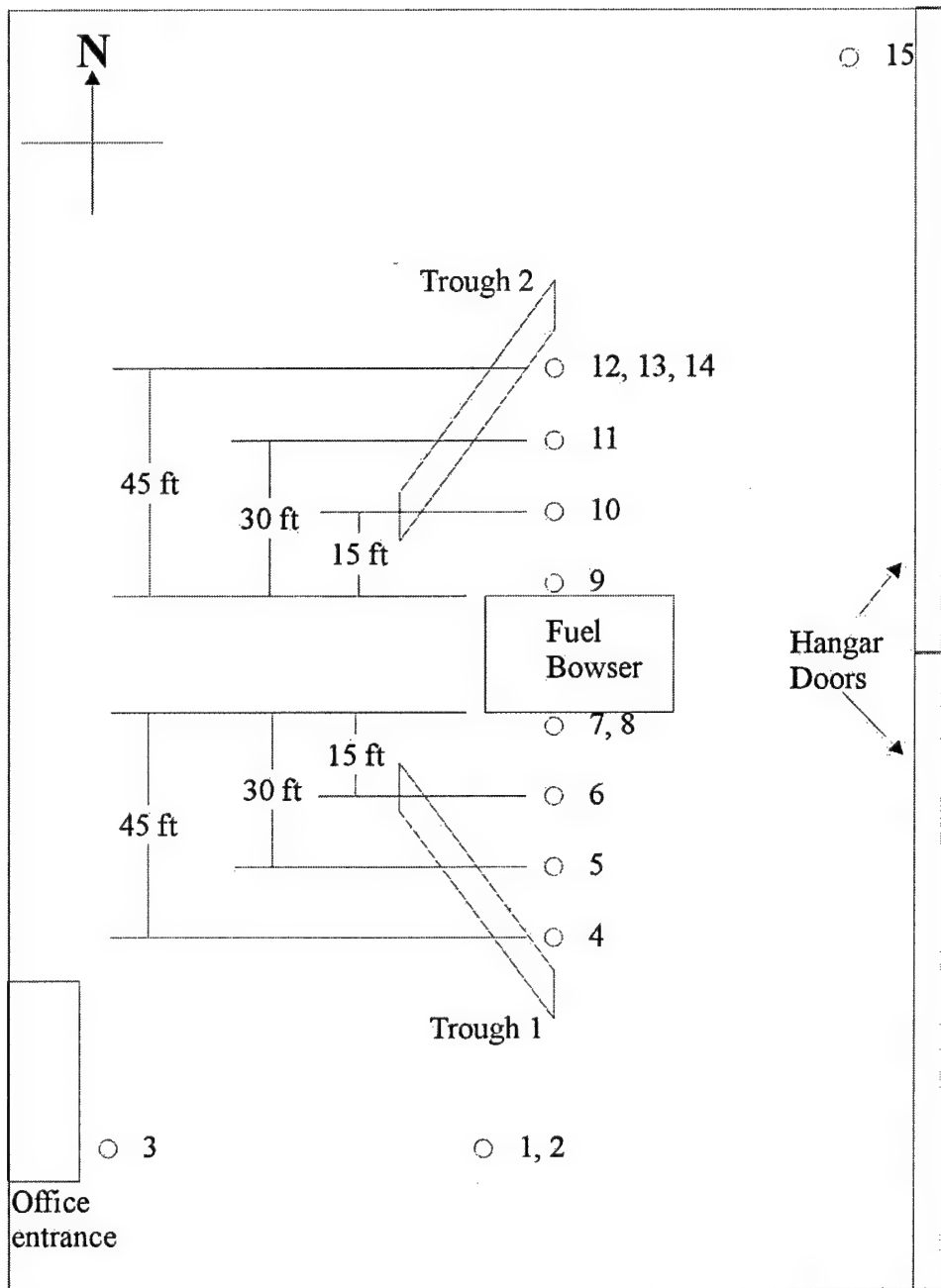


Figure 35. Locations where fuel vapor detector measurements were taken in building 976

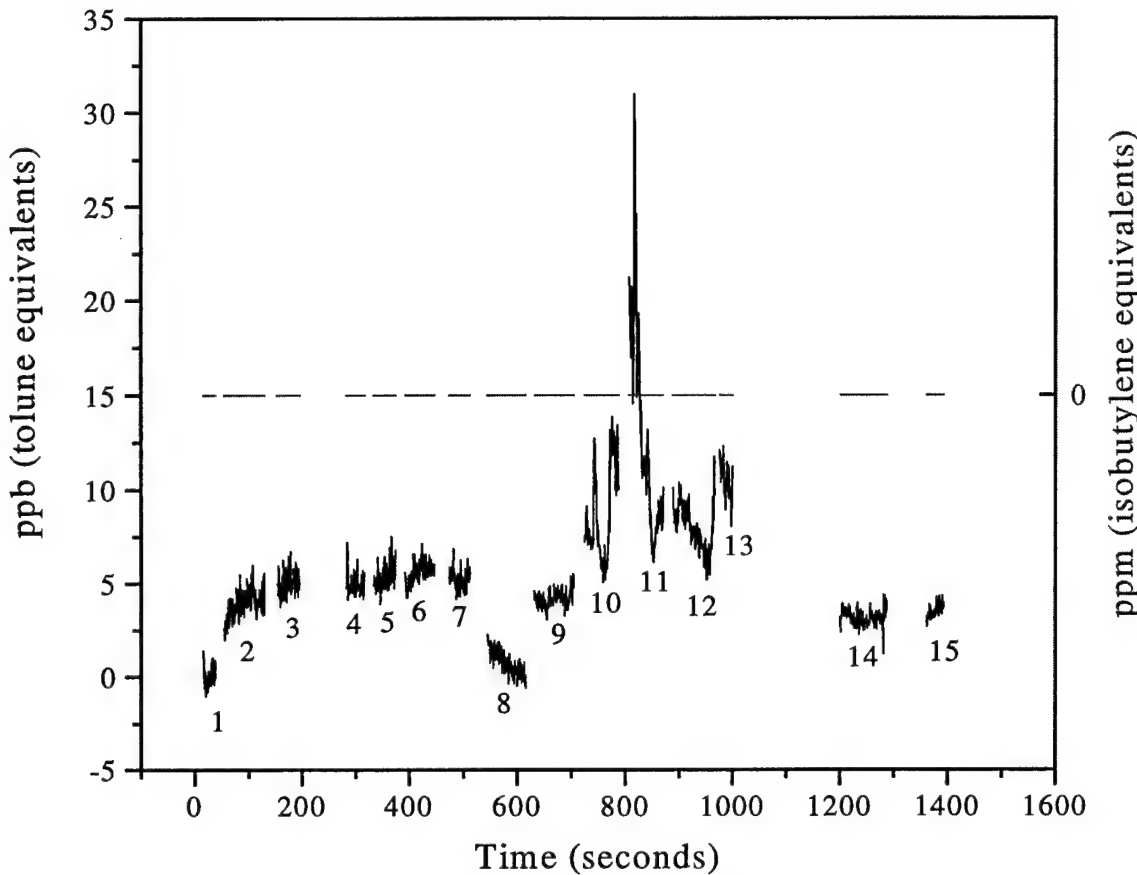


Figure 36. Fuel vapor detector logs in building 976

Below is a brief description of the results at each location:

- Log 1: Carbon scrubbed air signal, approximately 0 ppb toluene equivalents
- Log 2: Air above Trough 1, approximately 5 ppb toluene equivalents
- Log 3: Air near office door, approximately 5 ppb toluene equivalents
- Log 4: 45 feet south of fuel bowser, approximately 5 ppb toluene equivalents.  
Measurement of benzene concentration using a Draeger CMS unit was <0.2-ppm benzene
- Log 5: 30 feet south of fuel bowser, approximately 5 ppb toluene equivalents
- Log 6: 15 feet south of fuel bowser, approximately 5 ppb toluene equivalents
- Log 7: At south side of fuel bowser, approximately 5 ppb toluene equivalents  
Measurement of benzene concentration using a Draeger CMS unit was <0.2 ppm benzene
- Log 8: Carbon scrubbed air at south side of fuel bowser, approximately 0 ppb toluene equivalents
- Log 9: At north side of fuel bowser, approximately 5 ppb toluene equivalents

- Log 10: 15 feet north of fuel bowser, between 5 - 12.5 ppb toluene equivalents.  
Measurement of benzene concentration using a Draeger CMS unit was <0.2-ppm benzene
- Log 11: 30 feet north of fuel bowser, between 7 - 32 ppb toluene equivalents
- Log 12: 45 feet north of fuel bowser, between 5 - 10 ppb toluene equivalents
- Log 13: 45 feet north of fuel bowser, second time, 10 ppb toluene equivalents
- Log 14: Carbon scrubbed air 45 feet south of fuel bowser, approximately 2 ppb toluene equivalents
- Log 15: Northeast corner of building, approximately 2 ppb toluene equivalents

The locations that the fuel vapor detector measured BTEX levels above baseline levels were between 30 to 45 feet north of the fuel bowser. It is interesting to notice the spikes in signal at these locations, presumably due to "tendrils" of jet fuel vapor that are making their way around the building.

### **Building 230**

The fuel vapor detector was deployed in building 230. This building is on the north side of the parking location of the E-3 surveillance aircraft and fills with fuel exhaust fumes when the wind is from a southerly direction. Several areas of this building were measured with the fuel vapor detector, a Draeger CMS unit equipped with benzene analyzer chips and an indoor air quality monitor while an E-3 was running outside. During these measurements the wind direction was southerly with speeds averaging 11 knots (12-13 mph), which are the conditions when exhaust fumes are at their worst.

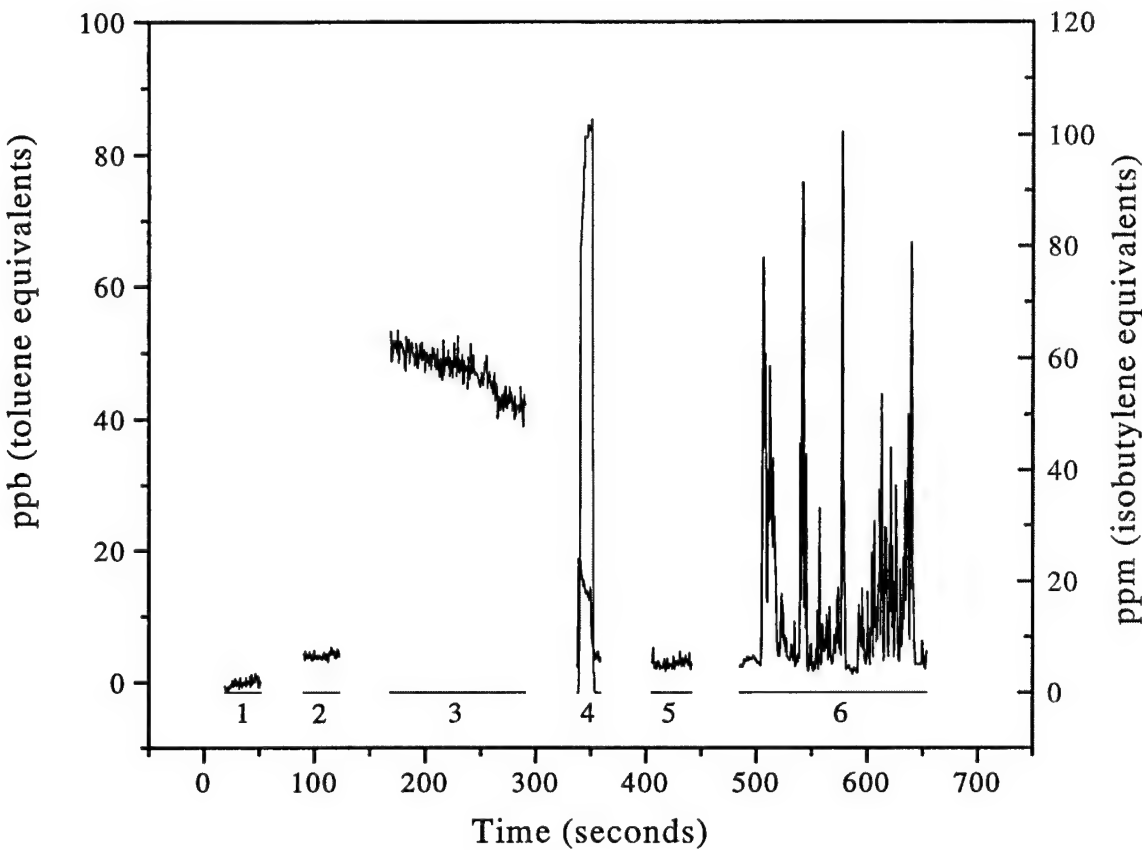


Figure 37. Fuel vapor detector log in pnedraulics room of building 230

Below is a description of the results from the pnedraulics room prior to powering up E-3 aircraft:

- Log 1: Carbon scrubbed air, approximately 0 ppb toluene equivalents
- Log 2: Pnedraulics room background signal, approximately 5 ppb toluene equivalents.  
Measurement of benzene concentration using a Draeger CMS unit was < 0.2-ppm benzene
- Log 3: Permeation tube calibration, approximately 50 ppb toluene equivalents
- Log 4: Isobutylene calibration of PID, approximately 100 ppm isobutylene equivalents
- Log 5: Background
- Log 6: Extension tube used to "sniff" around overhead door in pnedraulics room, between 5-85 ppb toluene equivalents measured.

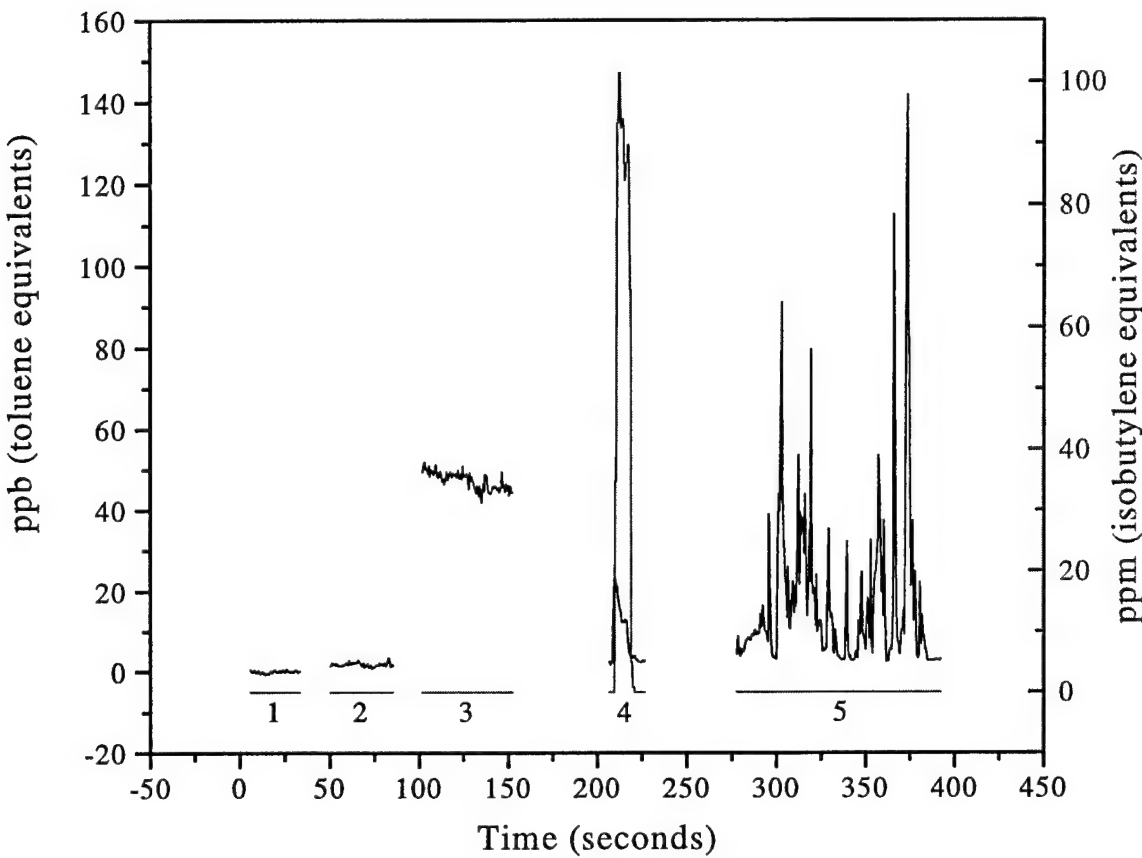


Figure 38. Fuel vapor detector log in computer room/study lounge of building 230

Below is a description of the results from the computer room/study lounge prior to powering up E-3 aircraft:

- Log 1: Carbon scrubbed air, approximately 0 ppb toluene equivalents
- Log 2: Computer room background signal, approximately 0 ppb toluene equivalents  
Measurement of benzene concentration using a Draeger CMS unit was < 0.2-ppm benzene. Indoor air quality monitor readings: CO<sub>2</sub> = 590-700 ppm; Relative Humidity = 31.4; Temperature = 61.5° F; CO = 0 ppm.
- Log 3: Permeation tube calibration, approximately 50 ppb toluene equivalents
- Log 4: Isobutylene calibration of PID, approximately 100 ppm isobutylene equivalents
- Log 5: Extension tube used to "sniff" around overhead door in computer room, between 5-140 ppb toluene equivalents measured.

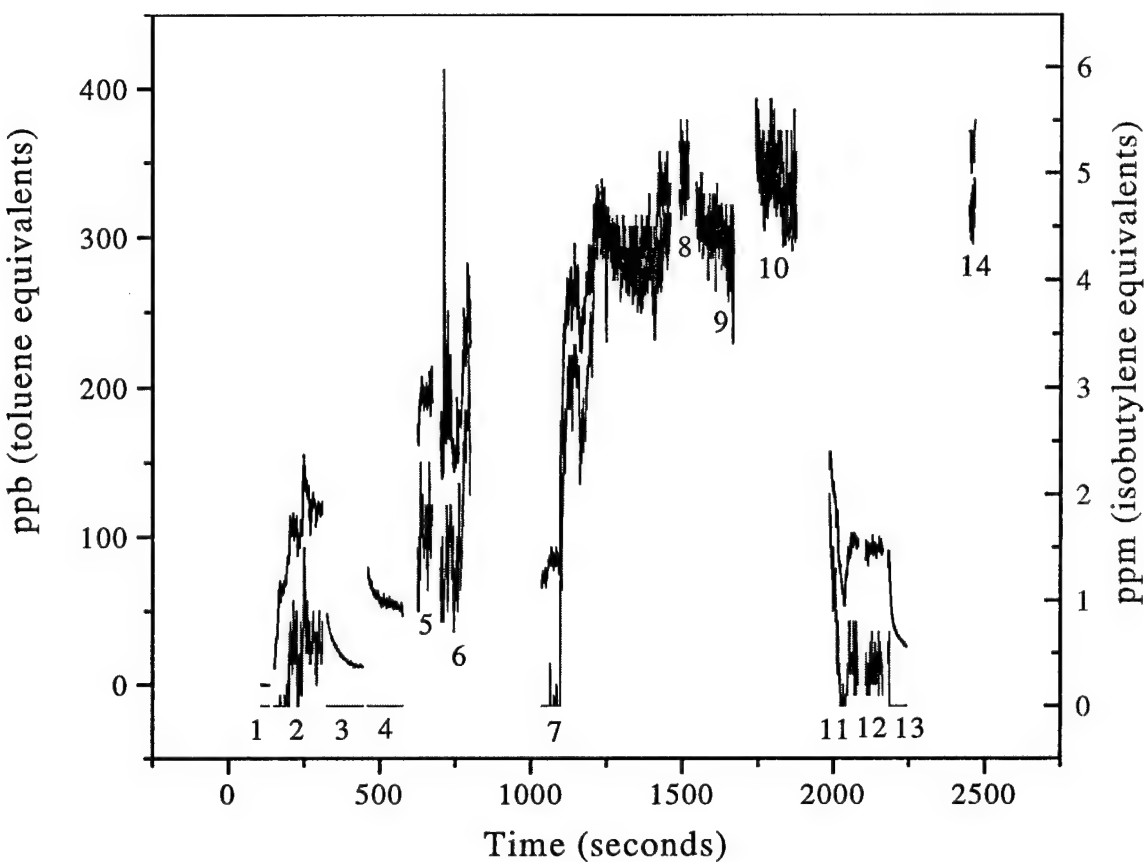


Figure 39. Fuel vapor detector log as E-3 is powered up. Also shown are logs as fuel vapor detector is moved around building 230.

Below is a description of the results while the E-3 aircraft was running:

- Log 1: Carbon scrubbed air, approximately 0 ppb toluene equivalents. Measurement of benzene concentration using a Draeger CMS unit was < 0.2-ppm benzene
- Log 2: Initial power up of E-3 aircraft. Signal ranged from 0 ppb initially to 150 ppb toluene equivalents as aircraft was powered up.
- Log 3: Carbon scrubbed air; signal dropped to approximately 5 ppb toluene equivalents.
- Log 4: Permeation tube calibration, approximately 50 ppb toluene equivalents
- Log 5: Computer room signal, approximately 200 ppb toluene equivalents. PID signal approximately 1.5-ppm isobutylene equivalents. Indoor air quality monitor readings: CO<sub>2</sub> = 700 - 800 ppm; Relative Humidity = 30.9; Temperature = 66.4° F; CO = 8-9 ppm.
- Log 6: Extension tube used to "sniff" around overhead door in computer room, between 150-400 ppb toluene equivalents measured. PID signal approximately 1.5 – 3.5 ppm isobutylene equivalents. Measurement of benzene concentration using a Draeger CMS unit was < 0.2-ppm benzene. Indoor air quality monitor readings: CO = 18 ppm.

- Log 7: Moving through hallway, at 1291 seconds moved past CRS conference room. Measured approximately 300 ppb toluene equivalents with fuel vapor detector. PID signal level of 4 ppm isobutylene equivalents. Indoor air quality monitor readings: CO = 16 ppm.
- Log 8: Radar Training sector (main hallway) signal levels of 350 ppb toluene equivalents. PID signal level of 5-ppm isobutylene equivalents. Measurement of benzene concentration using a Draeger CMS unit was < 0.2-ppm benzene.
- Log 9: Sergeant Ruth's office. Signal levels of 300 ppb toluene equivalents. PID signal level of 4.5-ppm isobutylene equivalents. Measurement of benzene concentration using a Draeger CMS unit was < 0.2-ppm benzene. Indoor air quality monitor readings: CO<sub>2</sub> = 960 ppm; CO = 17 ppm.
- Log 10: Radar/Computer support section room, signal levels of approximately 300 – 350 ppb toluene equivalents. PID signal level of 5 ppm isobutylene equivalents. Measurement of benzene concentration using a Draeger CMS unit was < 0.2-ppm benzene. Indoor air quality monitor readings: CO = 20 ppm.
- Log 11: Fuel vapor detector returned from Radar/Computer support room to pneumdraulics room.
- Log 12: By overhead door in pneumdraulics room, approximate signal levels of 100 ppb toluene equivalents. Indoor air quality monitor readings: CO<sub>2</sub> = 500 ppm; CO = 2 ppm.
- Log 13: Overhead door opened in pneumdraulics room, signal levels dropped to approximately 30 ppm toluene equivalents.
- Log 14: Fuel vapor detector returned to Radar/Computer support hallway, approximate signal levels of 300 ppb toluene equivalents. PID signal levels of 5.3 ppm isobutylene equivalents.

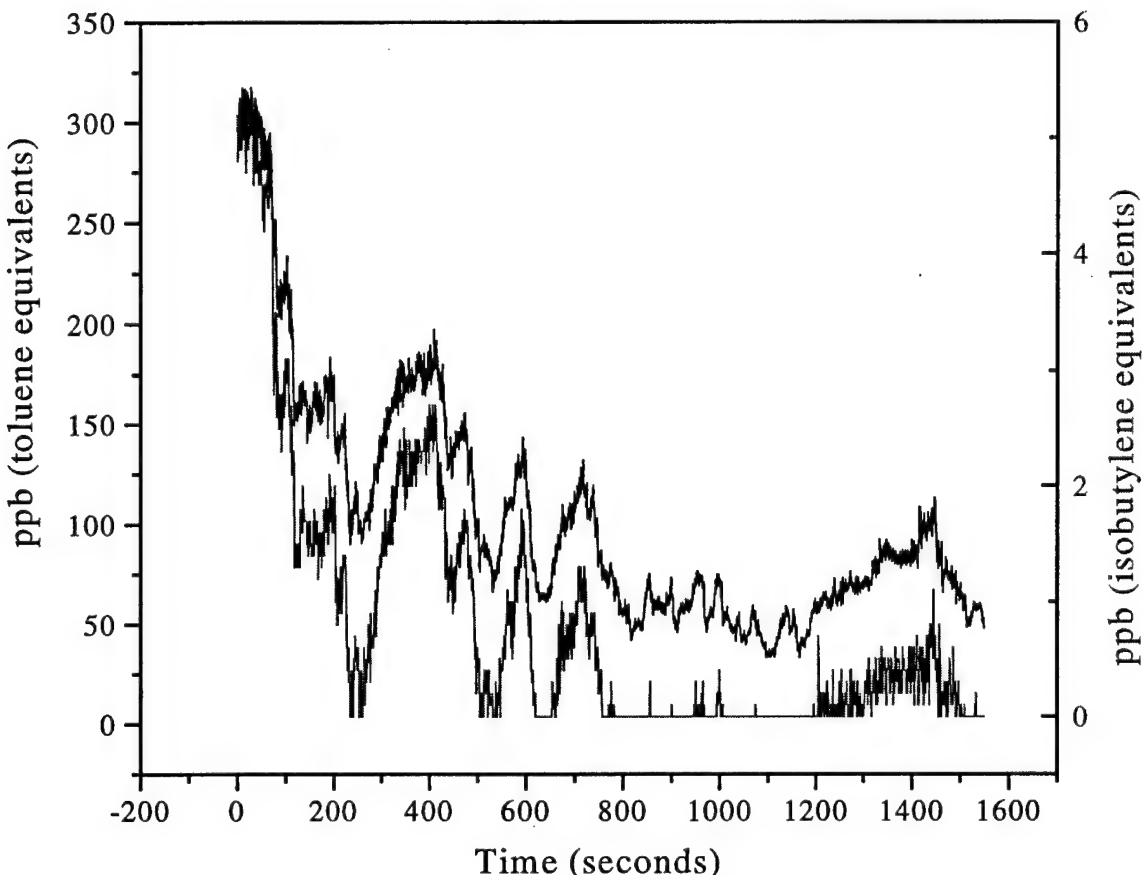


Figure 40. Fuel vapor detector log in building 230 after E-3 is powered down.

After the E-3 aircraft was powered down, the signal levels inside the Radar/Computer support hallway slowly dropped off. The outside door at the end of the hallway being opened caused the sharp drops in signal levels. Thirty minutes after the E-3 was powered down the indoor air quality monitor registered CO levels of 9 ppm.

### Spin-Off Applications

#### Aromatic Specific Laser Ionization Detector

After performing many of the laboratory studies with the leak detector prototypes, DTI recognized the high probability that a commercial gas chromatography (GC) detector could be developed on the basis of the REMPI technology and the low cost microchip lasers under development at Northrop Grumman. DTI collaborated with Professor Orven Swenson of the NDSU physics department on the writing of a Phase I SBIR proposal to the National Science Foundation in January 2001. The proposal was funded, and the Phase I work was carried out from July 2001 through March 2002. The proof of concept research was very encouraging, and DTI plans on submitting the follow-on Phase II proposal in July 2002.

The REMPI-based GC detector has been dubbed ArSLID (Aromatic Specific Laser Ionization Detector), and like the leak detector, it is both highly sensitive and selective towards aromatic hydrocarbons. The main difference between the leak detector and the ArSLID is the choice of laser. The microlaser used by ArSLID has much lower pulse energies than either the diode-pumped Diva or the flashlamp-pumped Big Sky Ultra used with the leak detector, which results in a loss of sensitivity. However, the price and size benefits of the microlaser are much more appropriate for this type of application. In addition, the high pulse repetition rate of the microlaser (~3 kHz) is beneficial for fast-GC applications. The chromatograms shown below illustrate the type of performance that was achieved during the Phase I effort.

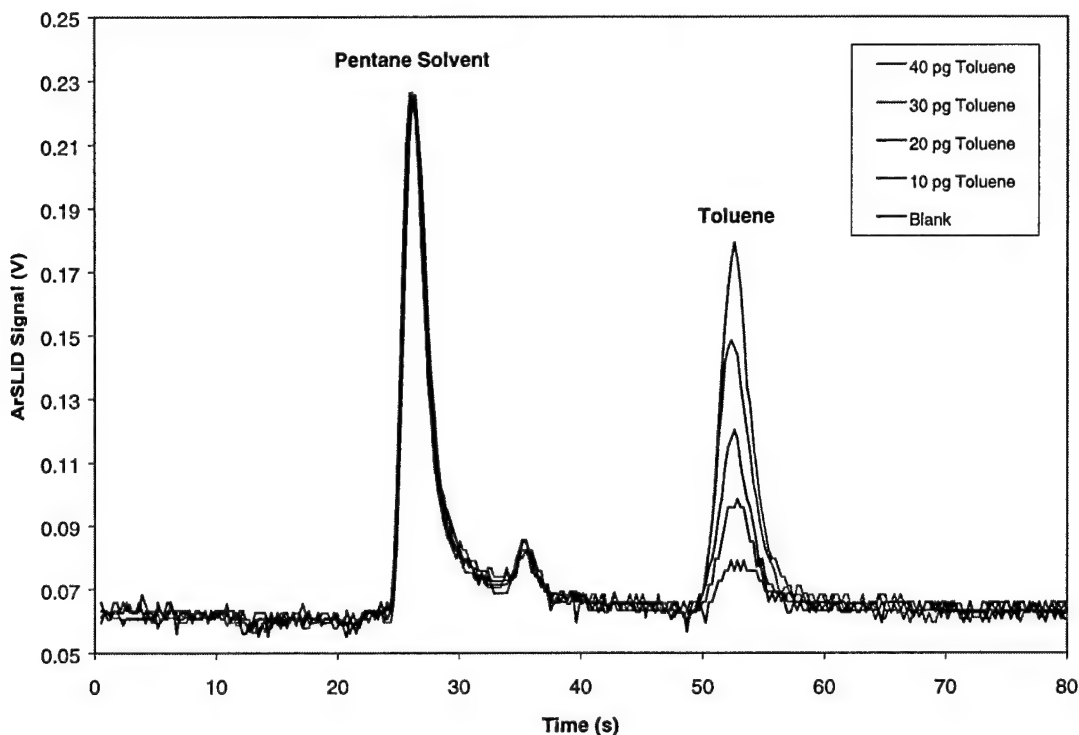


Figure 41. Sensitivity of ArSLID towards toluene

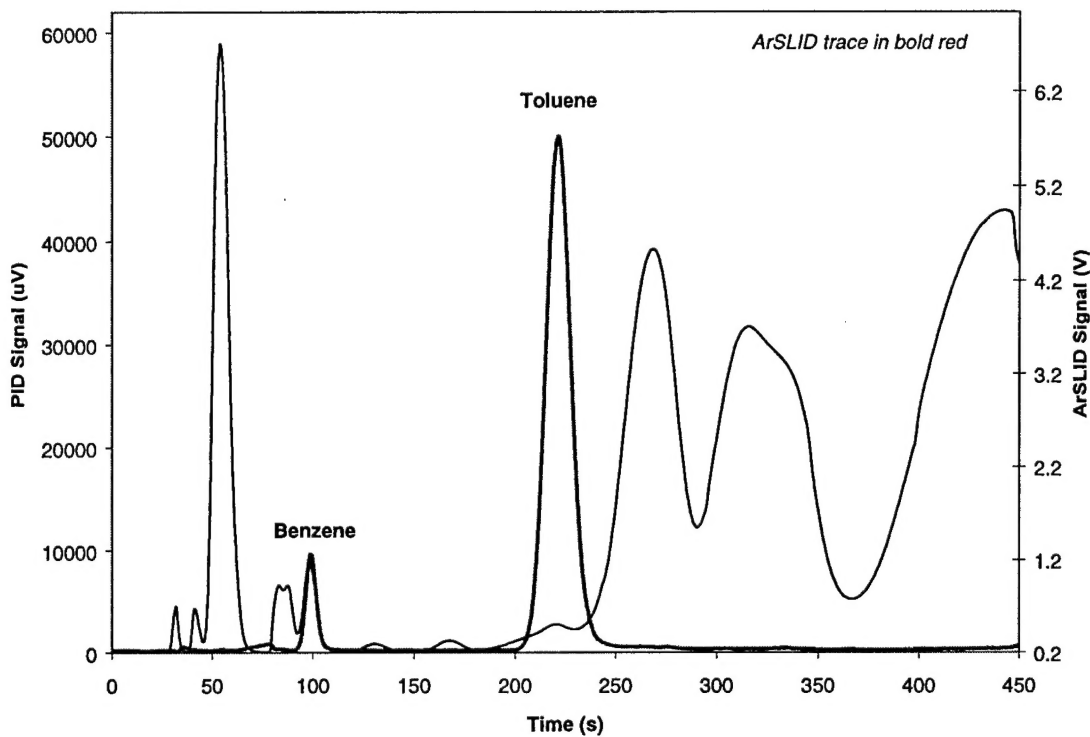


Figure 42. Selectivity advantage of ArSLID vs. PID for a mixture of aromatic and aliphatic hydrocarbons

#### Chemical Warfare Agents

We received an additional \$25K as a contract modification in September 2000 to investigate the utility of REMPI as a real time chemical agent detector. We applied laser ionization detection in ambient air to two chemical nerve agent simulants, dimethyl sulfide (DMS), an organosulfide, and dimethyl methylphosphonate (DMMP), an organophosphonate. Syage et al of Aerospace Corporation have previously studied the ultra-trace detection of chemical warfare agent simulants including DMS and DMMP.<sup>i,ii</sup> They used the technique of supersonic molecular beam; resonance enhanced multiphoton ionization, and time-of-flight mass spectroscopy (MB/REMPI/TOFMS). The purpose of our work was to demonstrate that similar results could be produced with simple field-able, ambient pressure, laser ionization detection (LID). Our results indicate that application to DMMP will be challenging due to the lack of an intermediate resonance state. The results for DMS are much more promising.

After completing the work on the modification and inspired by the events of September 11, 2001 we reinvestigated the opportunity to develop a chemical warfare agent detector. We procured a pure sample of Malathion (a common organophosphate pesticide) to act as a simulant for VX. This was chosen based on a report on the spectroscopy of chemical agents and simulants.<sup>iii</sup> We were initially extremely excited about the results obtained: sub-ppb limits of detection in real time. However, we recently learned that our Malathion sample was not as pure as reported and a contaminant was responsible for the results obtained.

This represents a small setback in the development of a chemical warfare agent detector. However, based on the published spectroscopy of the compounds, using a shorter wavelength of light (~213 nm; 5<sup>th</sup> harmonic of Nd:YAG) compared to what we use for the fuel vapor detector should provide a successful means to ionize chemical agents. We will be pursuing a broad agency announcement by Tyndall Air Force Base to obtain funding to develop the chemical warfare agent detector.

### *Oil and Gas Exploration*

Another potential spin off application is in oil and gas exploration. Gerry Calhoun and James Hawkins of New Paradigm Explorations in Midland, TX have developed a technique for oil exploration that involves measuring the BTEX concentration in near surface soil gas. With their technique, they bore a hole approximately ¾" in diameter and 18" deep in the ground. They seal the hole with an inflatable packer and draw a 100 mL sample of soil gas into a syringe and inject the sample into a miniature GC for analysis. Typical background levels for benzene and toluene are in the 50 ppb range. Areas that have anomalously high levels (defined as twice background levels) have a high probability for oil production.

We have done some preliminary work with New Paradigm using the fuel vapor detector side by side with their technique and the results were modestly encouraging. We are considering pursuing Department of Energy funding to further develop the fuel vapor detector into a real time oil exploration tool.

### Fulfillment of Technical Objectives

Table 4 outlines the ten Technical Objectives of this Phase II contract and their significance. Each objective was addressed, and the results were discussed in preceding sections of this report.

Table 4. Summary of technical objectives and significance

#	Brief Description	Significance
1	Replace flashlamp-pumped Nd:YAG laser with diode-pumped lasers	Size reduction, battery power, specific detection of benzene, easier mobilization
2	Achieve LOD below 100 ppbv for JP-8 and below 30 ppbv for unleaded gasoline	Documents key performance advantages vs. PID under optimal conditions for PID
3	Benchmark prototype LIDs against PID for entire range of possible conditions	Documents much greater stability and immunity from interferences from LID vs. PID
4	Implement man-machine interface and on-line calibration	Important needs for reliable operation and user-friendliness
5	Demonstrate specific GC detection of aromatic hydrocarbons by NanoLaser	Immediate commercialization opportunity
6	Demonstrate 50-fold sensitivity improvement with sorbent interface	Improves detection limits for most sensitive applications, e.g., breath analysis
7	Detect pipeline leaks too small to be seen by pressure testing	Solves important AF need revealed in Phase I; proves capability superior to existing methods
8	Perform extensive indoor air quality study in building 230 at Tinker AFB	Model for indoor air studies with new technology; help solve longstanding problems
9	Evaluate selected spin-off applications	Background for Phase III funding, other SBIRs
10	Document cost savings	Preparation for commercialization, Phase III

### Conclusions

This research project was very successful. We substantively met the technical objectives outlined in our initial Phase II proposal. We developed a real-time fuel vapor detector that is capable of portable field use. Applications we investigated as part of the research project were fuel pipeline leak detection, indoor air quality monitoring, and soil gas surveys for trace quantities of aromatic hydrocarbons.

The project is also positioned well for commercial success. We have contracted with the Air Force Center for Environmental Excellence (AFCEE) to develop a REMPI based fuel vapor detector that they can couple with a subsurface probe to locate and monitor fuel in groundwater and soil vapors. This will be an important tool in determining how far fuel has migrated in the subsurface relative to the initial discharge point. The sensitivity of REMPI will allow them to monitor the fuel near the maximum allowed concentration level without the need for extensive preconcentration of the vapors.

We have also submitted a proposal to AFCEE that will allow us to further develop the tools necessary to quickly locate leaks in buried pipelines and fuel tanks. This will represent the next and final step in the development of a pipeline leak detector. In Phase II we developed simple

yet effective tools that allowed a highly trained user to probe for leaks. In the AFCEE program we will transition to more advanced probes and simplify the man/machine interface such that a minimally trained user can operate the tool.

These fuel vapor detection opportunities, when coupled with the spin-off applications of Aromatic Specific Laser Ionization Detector for GC applications, chemical warfare agent detection, and oil and gas exploration have great potential for commercial success.

## References

---

i Jack A. Syage, James E. Pollard, and Ronald B. Cohen, "Ultrasensitive detection of atmospheric constituents by supersonic molecular beam, multiphoton ionization, mass spectroscopy," *Applied Optics*, **26**, 3516-3520 (1987).

ii J. S. Syage, J. E. Pollard, and R. B. Cohen, *Ultratrace Detection of Chemical Warfare Agent Simulants Using Supersonic Molecular Beam, Resonance Enhanced Multiphoton Ionization, Time-of-Flight Mass Spectroscopy*, Space Division Report SD-TR-88-13 (1988).

iii. Robert T. Rewick, Mary L. Schumacher, and Daniel L. Haynes, "The UV Absorption Spectra of Chemical Agents and Simulants," *Applied Spectroscopy*, **40**, 152-156, (1986).